DENTAL MATERIALS 33 (2017) 599–620

Available online at www.sciencedirect.com

ScienceDirect

journal homepage: www.intl.elsevierhealth.com/journals/dema

ADM guidance—Ceramics: guidance to the use of fractography in failure analysis of brittle materials

Susanne S. Scherrer[a,*], *Ulrich Lohbauer*[b], *Alvaro Della Bona*[c], *Alessandro Vichi*[d], *Michael J. Tholey*[e], *J. Robert Kelly*[f], *Richard van Noort*[g], *Paulo Francisco Cesar*[h]

[a] *Division of Fixed Prosthodontics and Biomaterials, University Clinic of Dental Medicine, University of Geneva, Geneva, Switzerland*
[b] *Research Laboratory for Dental Biomaterials, Dental Clinic 1, University of Erlangen-Nuernberg, Erlangen, Germany*
[c] *Post-Graduate Program in Dentistry, Dental School, University of Passo Fundo, Campus I, BR 285, 99052-900, Passo Fundo, RS, Brazil*
[d] *Department of Medical Biotechnologies, University of Siena, Siena, Italy*
[e] *Research and Development Department VITA Zahnfabrik, Bad Saeckingen, Germany*
[f] *Department of Reconstructive Dentistry and Center for Biomaterials, University of Connecticut Health Center, Farmington, USA*
[g] *School of Clinical Dentistry, University of Sheffield, Sheffield, UK*
[h] *Department of Biomaterials and Oral Biology, School of Dentistry, University of São Paulo, Brazil*

ARTICLE INFO

Article history:
Received 13 February 2017
Accepted 9 March 2017

Keywords:
Fractography
Ceramic
Zirconia
Fracture
Strength
Toughness
Wear
Fatigue
Interface
Failure

ABSTRACT

Objectives. To provide background information and guidance as to how to use fractography accurately, a powerful tool for failure analysis of dental ceramic structures.
Methods. An extended palette of qualitative and quantitative fractography is provided, both for in vivo and in vitro fracture surface analyses. As visual support, this guidance document will provide micrographs of typical critical ceramic processing flaws, differentiating between pre- versus post sintering cracks, grinding damage related failures and occlusal contact wear origins and of failures due to surface degradation.
Results. The documentation emphasizes good labeling of crack features, precise indication of the direction of crack propagation (dcp), identification of the fracture origin, the use of fractographic photomontage of critical flaws or flaw labeling on strength data graphics. A compilation of recommendations for specific applications of fractography in Dentistry is also provided.
Significance. This guidance document will contribute to a more accurate use of fractography and help researchers to better identify, describe and understand the causes of failure, for both clinical and laboratory-scale situations. If adequately performed at a large scale, fractography will assist in optimizing the methods of processing and designing of restorative

* *Corresponding author.*
E-mail addresses: susanne.scherrer@unige.ch (S.S. Scherrer), ulrich.lohbauer@fau.de (U. Lohbauer), dbona@upf.br (A. Della Bona), alessandrovichi1@gmail.com (A. Vichi), m.tholey@vita-zahnfabrik.com (M.J. Tholey), kelly@uchc.edu (J.R. Kelly), r.vannoort@sheffield.ac.uk (R. van Noort), paulofc@usp.br (P.F. Cesar).
http://dx.doi.org/10.1016/j.dental.2017.03.004

materials and components. Clinical failures may be better understood and consequently reduced by sending out the correct message regarding the fracture origin in clinical trials.

1. Foreword

First, the authors would like to make it clear that this paper by no means seeks to repeat or replace any of the current standards [1–3] or published books that have marked the field of fractography and failure analysis [4–8]. The National Institute for Standards and Technology (NIST) recommended practice guide by George Quinn, which has been recently updated, contains all the information needed for a fractographer to perform good descriptive (qualitative) and quantitative fractography and is available online at no cost [8].

This paper intends to provide selected guidance to assist any researcher who is starting to use dental fractography for in vitro or clinical failures in documenting and reporting the relevant findings appropriately. The focus of this paper as presented is on fractographic principles observed on brittle facture planes, as found in ceramics. Fractography of resin composites lies beyond the scope of this guidance project. Currently, the quality of the information delivered in the literature varies significantly, depending on the level of expertise of both the researcher and the reviewer. These guidelines therefore should help researchers to adopt a more standardized methodology for reporting fractographic data, especially within the dental literature, so that the discussions and conclusions drawn are fully supported by a thorough fractographic analysis. Specific documented examples of fracture origins identified on both in vitro specimens and in vivo restorations or replicas will reinforce the key role played by fractography in the dental field in relation to quality control, processing, prosthesis design, surface grinding damage, and in situ surface wear degradation. The examples presented herein are meant to open a new analytical dimension to strength-testing papers and studies dealing with clinical complications (survival and success rates) that usually list the existing fractures or chippings but rarely perform any type of fractographic failure analysis. With the currently available knowledge delivered through standards, books, scientific articles, and hands-on training courses, the dental community still needs to become more involved in applying this powerful analytical tool accurately.

2. Introduction

The first use of clinical fractography in the dental literature involving ceramic clinical failures goes back to 1989 and 1990, when Kelly et al. started to analyze fracture surfaces of failed all-ceramic dental restorations with the objective of finding the fracture origin [9,10]. Since then, the use of fractography has increasingly grown particularly in the past 10 years for both in vitro lab-scale specimens or in vivo ceramic restorations. Fractography is a powerful tool that allows for an accurate failure analysis based on the interpretation of microscopic fracture surface features that reveal the direction of crack propagation, pointing back to the origin or cause of failure. Fractography can be performed in a qualitative or descriptive way by means of recognition of surface crack features that indicate the direction of crack propagation. This method is mostly used in clinical failure analysis [8,11–29]. Quantitative fractography is applied in materials engineering studies and provides quantitative measurements of fracture surface features, particularly the critical flaw (origin), which has a specific shape and size and is used to determine the fracture toughness or the fracture stress based on fracture mechanics relations [30–32]. Such quantitative evaluation has been applied to fractured clinical ceramic restorations, allowing determination of flaw sizes and estimation of failure stresses [17,28,29,32,33]. Fractures may occur from critical stress concentrations, cyclic fatigue assisted by stress corrosion (slow crack growth), or from a combination of mechanisms involving processing methods and restoration design. Interpretation of clinical failures is not always straightforward as it is highly dependent on the available recovered parts and on the ceramic microstructure, glasses being easier to analyze than polycrystalline ceramics. Nevertheless, if the fractographic analysis is accurately performed, the information obtained may disclose relevant processing or design problems and then, measures can be taken to avoid similar failures in the future. The findings obtained from fractography have a key role to play in the mechanical performance of the product, the development or improvements of materials, in the manufacturing and design, in the handling, laboratory grinding adjustments and finishing/polishing procedures. The dental materials researcher, while testing existing products or new materials under development, can help to raise awareness of potential causes of failure and provide the necessary feed-back to all the actors involved.

Both descriptive and quantitative fractography should be part of research projects in which ceramic fracture is involved, whether during testing or clinical trials. The selected examples in this paper will show the various applications of fractography as a valuable and necessary tool to perform failure analysis on fractured surfaces of dental ceramics. Along this text the reader will find documentation regarding critical flaw identified on the fractured parts of dental ceramic in different testing conditions, such as flexural strength, fracture toughness, multilayer interfaces, thermal stress, fatigue, clinical use and wear.

3. Qualitative fractography (in vitro)

Qualitative fractography is performed by means of optical tools such as a stereo microscope, SEM, Field emission—SEM usually combined with Energy Dispersive X-ray spectroscopy

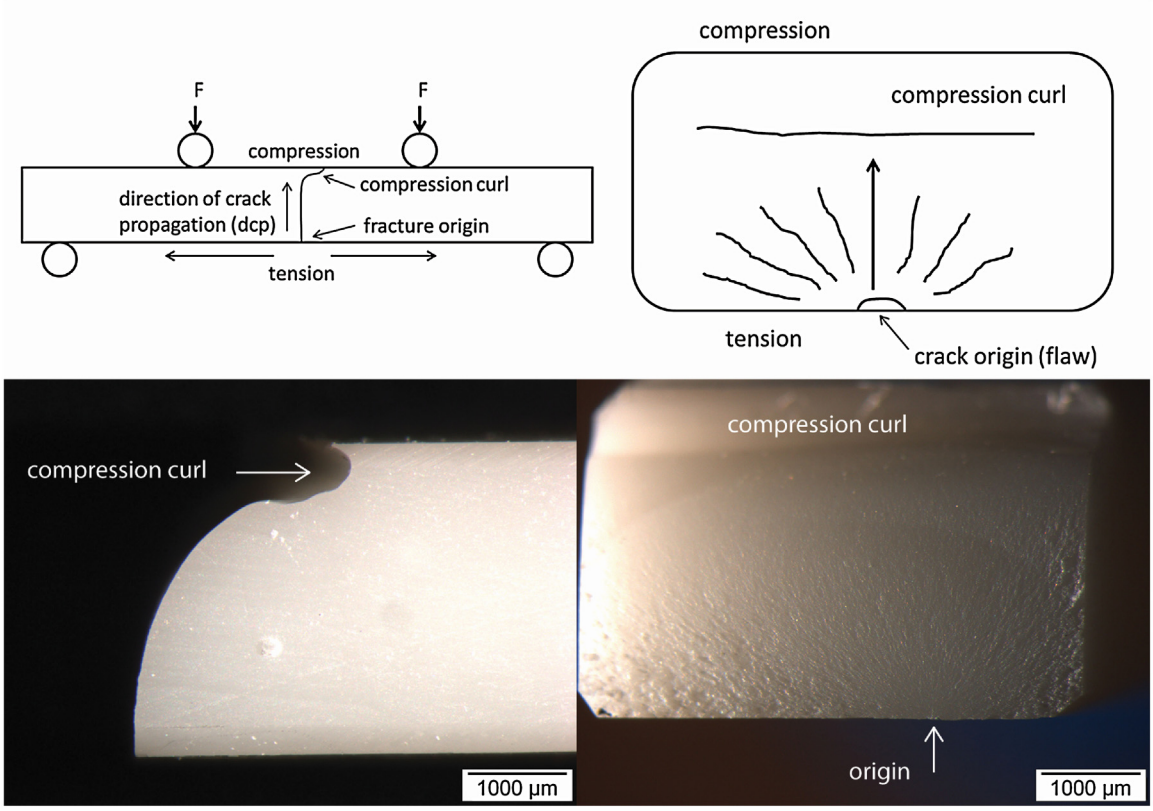

Fig. 1 – Schematic and illustration of a zirconia bend bar under 4-point flexure test. The fracture origin is to be searched on the tensile side. A compression curl is usually easy to see and will be located at the compression side. The two stereomicroscope images show a side view (left) and fracture surface (right) of the broken zirconia bend bar.

(EDX) in case of a localized need for elemental identification. Detailed reading on tools and equipment can be found in George Quinn's practice guide of fractography [8].

3.1. *Origins in strength testing*

Ceramics are known to have a brittle behavior, with only approximately 0.01% of elastic elongation and no detectable plastic deformation. Therefore, linear elastic fracture mechanics (LEFM) is applicable to ceramics and describes stresses at crack tips, slow and fast crack growth and catastrophic failure when the stress states have exceeded the materials' fracture toughness. Identification of crack origins from which the fracture started to propagate can provide valuable information every time new material developments or designs are created. Determination of relevant mechanical properties such as (i) fracture toughness (K_{Ic}), relating defect size and stress at failure, (ii) strength, for which a probabilistic approach using the weakest link distribution is involved, or (iii) fatigue testing establishing fatigue limits, will regularly include the use of fractographic analysis.

When carrying out a strength test with ceramic materials one needs to remember that all materials have an inherent population of defects (also called flaws) due to processing, which include powder composition (purity, homogeneity), powder compaction (pressing parameters, agglomerate size, powder friction), sintering (cracks and pores), presintered or solid state sintered ceramic machining and handling (scratches, edge chipping, cracks) [34]. These defects vary in size, shape, distribution and orientation. They are either volume distributed from the fabrication process (pores, large grains, inclusions) or surface distributed from surface treatment (precracks, edge chips, machining scratches or grooves) [34]. The material will fail when the nominal strength is overcome by the stress peak concentrated around a defect. An example of brittle fracture is shown in a zirconia bend bar (Fig. 1). The tensile side is at the bottom where the origin is found. A compression curl is at the top where the compression side is located. Flexure testing usually will show a compression curl on the opposite side to the failure origin. The very first approach using fractography of strength tested specimens is to orient the broken surface such as to have the tensile side at the bottom and compression side at the top. The compression curl is usually very easy to identify on bend bars and a quick stereomicroscope image with the right lateral illumination will highlight relevant fracture features including the area of the fracture origin (Fig. 1). Further SEM analysis (Fig. 2) at higher power will allow identification and characterization of the type of flaw responsible for failure.

Similar porous regions, as shown in Figs. 2c and 3 bc, are the result of interstices or pores remaining between agglomerates that underwent poor deformation during powder compaction. Zirconia grains that sintered freely in air (i.e. unconstrained sinter conditions) will have round shaped grains versus a more

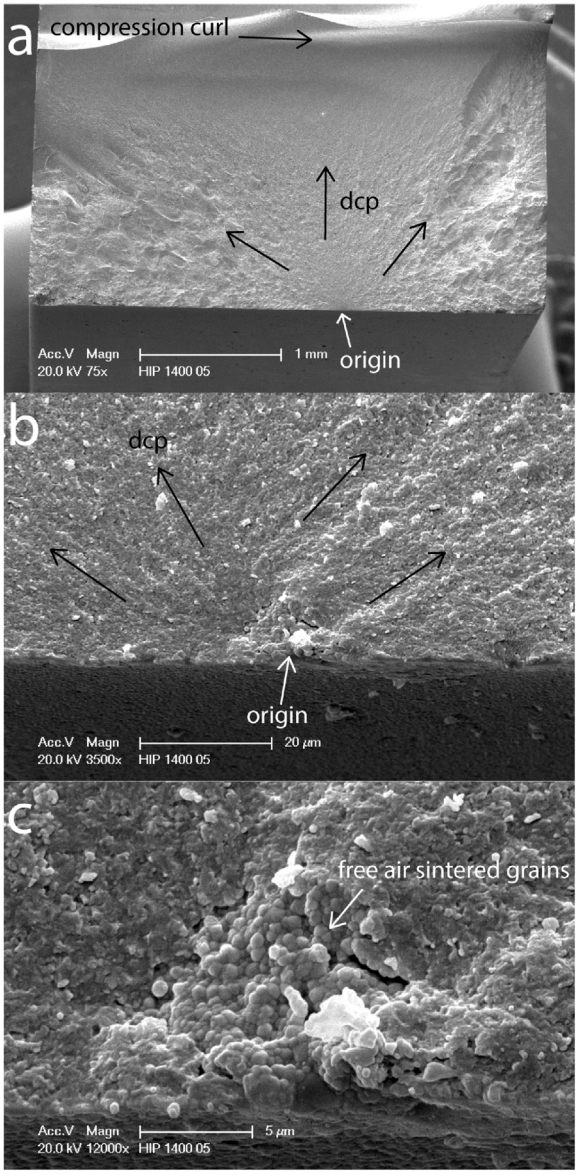

Fig. 2 – Standard documentation of a bend-bar strength-test failure. On the overview (a), the orientation of the specimen is labeled (compression curl on top), the direction of crack propagation (dcp), the origin (on the tensile side, bottom). The close-ups (b,c) of the origin should provide enough details with respect to volume, near-surface or surface generated flaws. (c) taken at 12,000× magnification shows the origin being a porous region (~10 × 10 μm) between agglomerates during compaction. The zirconia grains are free air sintered as seen from shape of the grains which are round versus the more angulated grains on the bulk fractured surface as a result of inter or transgranular fracture (data from Ref. [35]).

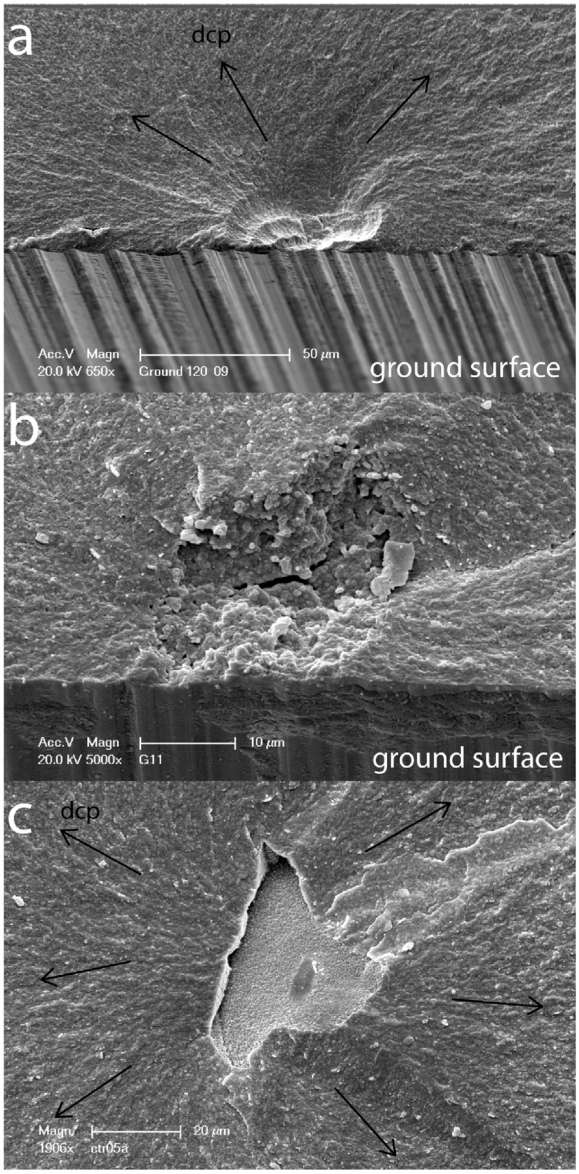

Fig. 3 – Critical flaws representing failure origins in lab-scale tested 3 Y-TZP bend bars. (a) shows a surface flaw from rough (120 μm) grinding on the tensile side of a specimen. Black arrows indicate the dcp based on fine hackle radiating outward; (b) shows a surface connecting origin of a porous region (20 × 25 μm) related to pressing powder agglomerates. Inside the porous region, the grains are free-air sintered (round); (c) shows a volume located origin from a large void defect between agglomerates or granules from powder pressing. The center of the defect shows again free sintered grains. Hackle are radiating from this pore outwards and indicated by black arrows for the dcp. All these defects are representative of processing issues (data from Ref. [35]).

angulated grain shape seen on the bulk fractured surface as a result of inter or transgranular fracture. The shape of the grains (round versus angled) may serve as a diagnostic tool during failure analysis and thus understand if the defect was introduced before or post sintering. An example is given in Fig. 4, which shows grinding cracks introduced in a zirconia bend bar in the presintered state. Later in this paper, grinding cracks in the presintered state resulting from reshaping zirconia CAD–CAM framework will be shown (Figs. 14 and 15).

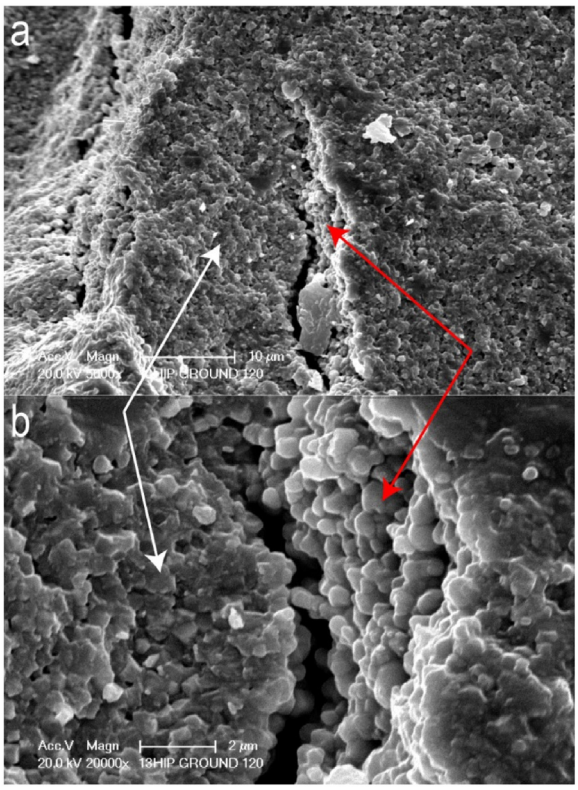

Fig. 4 – Fractured surface of a zirconia bend bar. The free-air sintered grains (within a fissure space) are round-shaped (red arrows) whereas the grains on a bulk fractured surface post-sintering are angulated in shape as a result of transgranular or intergranular fracture.

Recommendation1: When documenting and identifying critical flaws in strength tests (bend bars, biaxial discs), the fractographic analysis should provide an overall image (Figs. 1–3) of the broken part at low magnification so as to allow clear detection of both the tension and compression sides (signaled by a compression curl), as well as intermediate and high magnification images of the origin (Fig. 2b,c). Photographs should be labelled with the direction of crack propagation (dcp), the origin and all other key fracture surface features (fracture mirror, hackle, wake hackle, twist hackle, arrest lines, compression curl) to confirm the fracture orientation. A view at a slight angle showing simultaneously the fracture surface and the surface in tension is helpful in verifying if the origin is connected to the surface or near surface and if specimen processing (such as grinding, sandblasting) is related to the failure origin (Fig. 3a). The origins, which are of key interest in failure analyses, should also be photographed at high magnification (Figs. 2c and 3) in order to allow discussions regarding the type of flaw that was responsible for fracture.

3.2. *Origins labeled in Weibull or S–N graphs*

Specimens of the same ceramic material will not fail at one reproducible strength value but will have a strength distribution value based on their flaw population. The Weibull distribution is based on the theory that the largest structural defect in a loaded body controls it's strength [36]. The Weibull two parameter distribution contains a scale (σ_0) and a shape parameter (Weibull modulus, m). The scale parameter is called the characteristic strength σ_0 and corresponds to the 63.2% failure probability (see Fig. 5) whereas the Weibull modulus m indicates the homogeneity of the strength data, thus expressing reliability. A Weibull modulus in the range between 10 and 40 is related to ceramic materials with less variation during strength testing, i.e., a narrow flaw population and overall improved quality. A low m (between 1 and 10) means a wide distribution, large spread and low reliability, which requires improvement and thus a closer look at the reasons for failure. Generally speaking, increases in strength and reliability will come from a significant reduction in the critical flaw size by means of improvements made to the processing methods. A thorough and practical review of the Weibull analysis illustrating the importance of flaw size distributions when using different test configurations has been published by Quinn and Quinn [36]. The authors analyzed every single specimen and identified different failure mechanisms leading to clustered flaw populations. An important prerequisite for a thorough Weibull analysis is a sufficient number of specimens. A sound analysis is based on thirty or more samples in a group (EN 843-5). What is very helpful in the data analysis is to present a fractography montage in conjunction with a Weibull strength graph [1,8,37], or to follow-up with SEM fractographic analysis to show the type of flaws encountered during strength testing [38–41]. Overlooking the step of identification of the critical flaw population may lead to wrong conclusions when comparing reliability data between materials or when claiming that one ceramic is significantly stronger or weaker than another without understanding the causes of fracture. An example of a fractographic montage is given in Fig. 5.

Similarly to strength specimens, fatigue tested specimens should also be fractographically analyzed for critical flaw assessment. The type of flaw (ceramic processing or surface induced) can be labeled directly on the S–N plot (Fig. 6) and selected fractographic images of the critical flaws discussed to explain the findings. The early and high stress cycles may activate a different population of flaws compared to that activated in specimens cycled for longer times. In a S–N (Wöhler) fatigue study on 3Y-TZP [42], S–N data showed that processing defects (pressing of powder granules) were primarily activated under conditions of high stress/low cycle (<2000) fatigue, whereas the grinding surface flaws were the dominant ones when subjected to low stress/high cycle (from 2000 to 10^6) fatigue. Of course the location, size and shape of the critical flaw, whether intrinsic or from grinding, have to be considered, as well as the stress level and loading direction.

4. Quantitative fractography (in vitro)

Fracture toughness (K_{Ic}) expresses the material's resistance to unstable crack extension and is a design relevant material property. A separate ADM guidance document introduces the principles of fracture mechanics and fracture toughness [43]. Depending on the fracture mechanics literature the flaw size is denoted either "a" or "c". The following relationship $K_{Ic} = Y\ \sigma_f\ \sqrt{a}$ (Griffith Criterion, Eq. (1)) [1,8,44] describes the critical stress intensity factor, K_{Ic}, which is linked to a stress

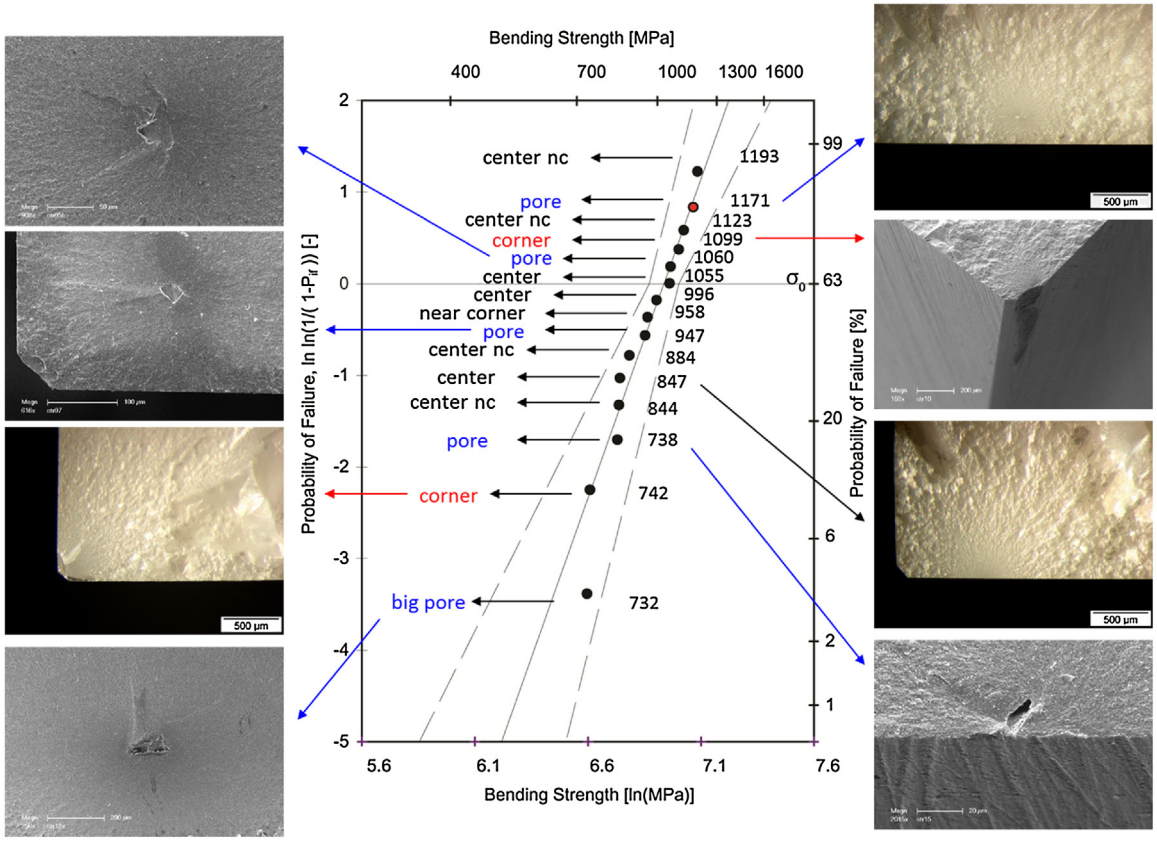

Fig. 5 – Example of a fractographic montage superimposed on a Weibull strength distribution with confidence intervals of 3Y-TZP bend bars. Failure origins of selected specimens within the Weibull distribution are shown in stereo and SEM images. Fracture origins are sintering pores and grinding damages, flaws at corners or near corners (nc) or pores located in the volume or near the surface resulting from the compaction process. The Weibull σ_0 = 1028 (963–1099) MPa shows a mix of specimen preparation problems and intrinsic processing defects, which contribute to a rather low reliability, as indicated by the m value of 6.97 (4.9–10.0) (data from Ref. [35]).
NB: Weibull estimates should be performed on a minimum of 30 strength data which was not the case in this example.

at failure (σ_f), a crack depth (a) and a stress intensity shape factor coefficient Y which will range between a value of 1.1 and 1.99 depending on the overall crack shape (width 2c and depth *a*). The crack depth can be precisely calculated [31,45] or approximated from crack depth over width (a/c) ratios [8,44]. One has however to be familiar with finding the origin using fractography and measuring the correct critical crack size for fracture toughness determination [17,31,32]. The extent of the critical flaw size *a* is defined by the area of the fracture mirror which is typically a smooth and semielliptical region around the fracture initiating defect [8]. Several fracture toughness tests exist and among them is the Surface-Crack in Flexure (SCF) [8,44], which requires specific crack size measurements using fractography. A few research papers in the dental literature have applied this test successfully [46–48] and have provided images to show the delineated critical crack size for fracture toughness calculation.

One interesting aspect of failure analysis is to work with the parameters in Eq. (1). Hence, toughness can be estimated from crack size and stress measurements [31] (Fig. 7), or stress can be estimated from crack size and known toughness values [49], or estimates of crack sizes can be given from known toughness and stress information when one has to find the fracture origin and wants some magnification scale information to search for it. However, it is important to keep in mind that the material needs to meet the requirements of LEFM, and that failure must have occurred from a remote stress field and in mode I (tensile crack opening). An example of chip damage induced from grinding and viewed on a mirror polished bonded interface is shown in Fig. 7. The chip depth is assimilated as a critical flaw of a crack size (a) (Eq. (1)). Fracture stress estimates were calculated from Eq. (1) based manufacturer's K_{Ic} and then extrapolated to potential losses of strength when comparing to the manufacturer's reported strength [49,50].

The well delineated fracture origin in Fig. 7 has a peculiar microstructure that differs from the bulk microstructure and corresponds to excessive grain growth. This is due to a localized concentration of 2.8 wt% of CaO used as a sintering catalyst and was detected by energy dispersive X-ray spectroscopy (EDX). This flaw, made of large grains, was the fracture origin and was responsible for the low fracture stress (680 MPa) in this 4-point bending fractured bend bar specimen. The critical flaw (a) measured 13 μm deep and 37 μm wide (2c). The calculated critical stress intensity shape factor Y_{depth} is

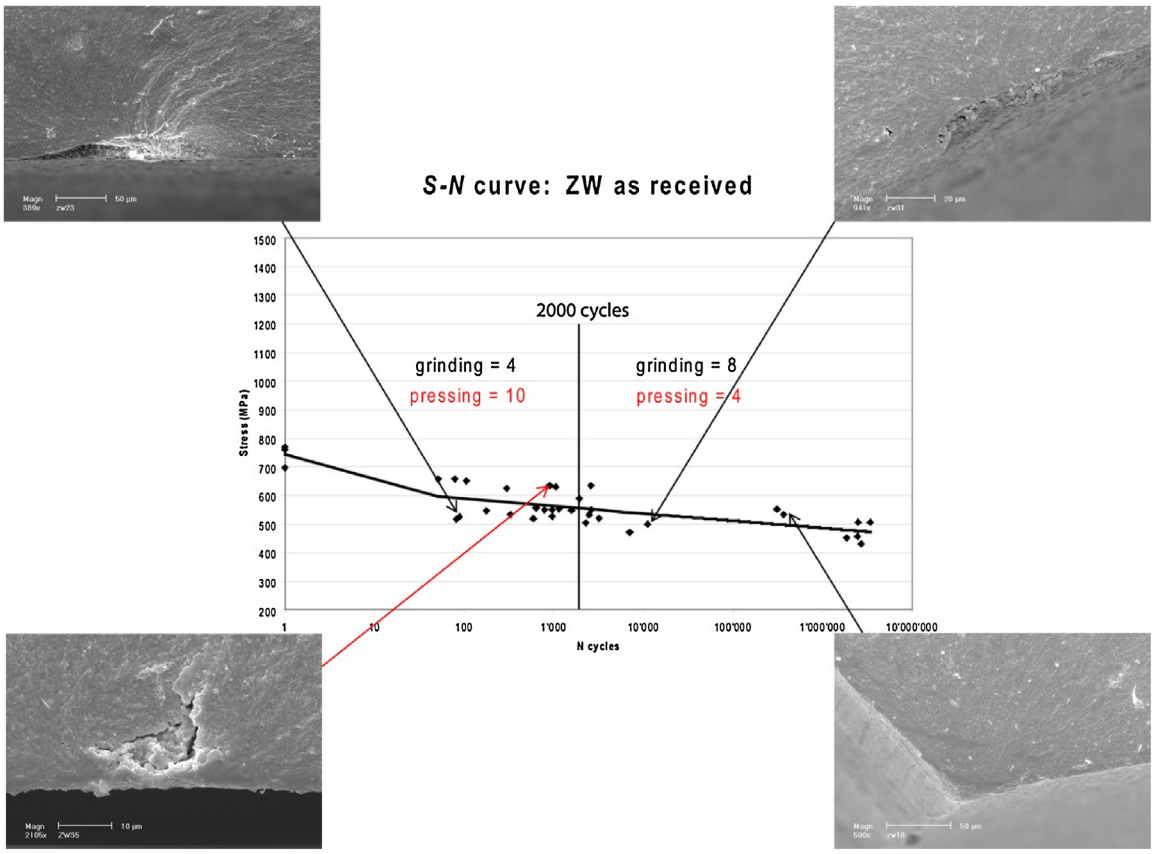

Fig. 6 – Example of fractographically labelled S–N data. Failure origins of selected specimens within the fatigue test are shown by SEM images. Location of fracture origins in bend bars are flaws from pressing, grinding or corner cracks (data from Ref. [42]). The red arrow is for a pressing defect on the S–N data points. (For interpretation of the references to color in this figure legend, the reader is referred to the web version of this article.)

Recommendation 2: Fractographically identified fracture origins are marked on the Weibull strength distribution plot (Fig. 5) or on a fatigue S–N curve (Fig. 6). Hence, the flaws responsible for failure can be differentiated between intrinsic to the ceramic (sintering pores, voids from compaction of granules or agglomerates, inclusions, impurities, etc.) or related to sample preparation (grinding, specimen preparation) and testing issues (Figs. 2 and 3). The weakest specimens should be analyzed with great interest as they represent early failures at stresses at the lower end of the distribution. Their critical flaws should be compared with those of the high strength specimens.

1.4 using solutions from Scherrer et al. [48]. Hence, the resulting fracture toughness using Eq. (1) would be in this case only 3.4 MPa$\sqrt{m}$ which is rather low compared to the usual value of approximately 4.5–5 MPa$\sqrt{m}$ reported for 3Y-TZP.

By using the backscattering mode in the SEM, it becomes often possible to highlight structure features and distinguish different phases, which can complement a first SEM image. As an example, Fig. 8 shows another zirconia specimen of the same research [35] with a failure origin from excessive grain growth similar to that seen in Fig. 7. The backscattering mode at 3500× reveals many large grains forming one large critical flaw activated during 4 point-bending. For this particular specimen, the fracture stress σ_f was 586 MPa, the measured critical flaw depth a = 20 μm and width 2c = 60 μm, the calculated Y_{depth} = 1.42 using Scherrer et al. [48]. Based on Eq. (1), the calculated K_{Ic} was 3.7 MPa$\sqrt{m}$. One explanation for such low toughness may be the additional processing step of post sintering Hot Isostatic Pressing (post-HIP) performed at 1400 °C for 2 h which, together with a 2.8 wt% of CaO, may have contributed to this localized grain growth.

The problem of contamination or detrimental chemical additives involved with the failure origin is illustrated in Fig. 9 to which EDX was added. Two failure origins from strength testing are documented in 3Y-TZP bend bars. The first one is a large pore at the failure site containing alumina particles, possibly from powder contamination. The second is a flaw containing a concentration of 2.8 wt% CaO, which contributed to localized grain growth, weakening the zirconia and from which the crack started (data from Ref. [35]).

5. Qualitative fractography (in vivo)

5.1. *Origin identification using a systematic approach*

As with lab-scale in vitro specimens, fractographic failure analysis has to be systematic in its approach. The very first

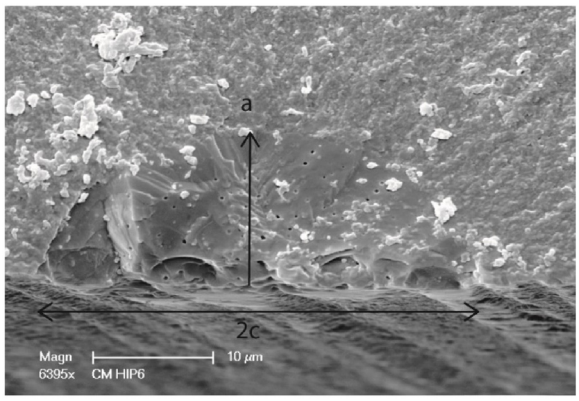

Fig. 7 – Fracture origin in a 3Y-TZP bend bar fractured in 4 point-bending. The critical flaw has a crack depth (a) = 13 μm, a crack width (2c) = 37 μm, a fracture stress (σ_f) = 680 MPa and a calculated critical intensity shape factor Y_{depth} = 1.4 using Scherrer et al. [48]. Hence, the estimated fracture toughness in this case would be K_{Ic} = 3.4 MPa$\sqrt{m}$ (data from Ref. [35]).

objective is to be familiarized with all the possible fracture surface features encountered in ceramics. The best available reference for that is the NIST recommended practice guide for fractography of glasses and ceramics by George Quinn [8]. Several clinical papers have since then used a systematic approach for clinically failed specimens [8,11–25,32] and it is gaining momentum within the dental research community but never or rarely [20] used in clinical trials when reporting ceramic survival or failure rates. The purpose in this guidance document however, is not to repeat the content of reference papers but to provide a relevant hints on the major help of using fractography when attempting to understand the reason for premature failure of a clinical component. The cause of failure usually goes back to design issues, processing induced damage (manufacturer, lab and clinician) or surface contact damage and material degradation from the mechanically harsh environment of the oral cavity (i.e., peak loading, cyclic loading, friction or abrasive wear, excessive contact pressure, bruxism, multidirectional chewing, off-center loading of implant supported ceramic restorations, water and temperature exposure, slow crack growth, aging). In most cases one would find a combination of the above listed factors involved in the fracture process.

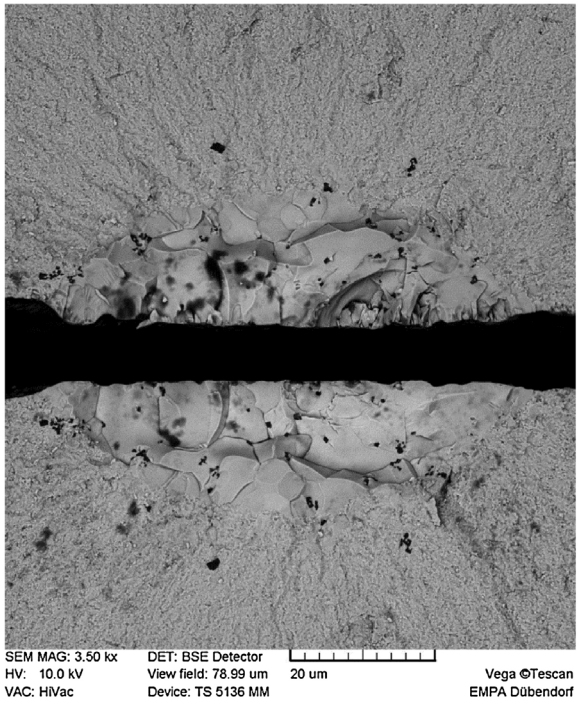

Fig. 8 – Backscatter viewing mode of a critical flaw made of excessive grain growth in a 3Y-TZP after post-sintering HIP and 4-point bending strength test.

For each clinical failure, maximum of information should be collected before starting the fracture analysis. These include: (1) intra-oral pictures to secure the anatomical orientation of the fracture, (2) crown number in the FDI system, (3) knowledge of the ceramic material (core, veneer), (4) time to failure, (5) circumstances of the fracture event as provided by the patient, (6) retrieval information by the clinician (including cementation/adhesive luting procedures). Further documentation by the fractographer will include stereo microscopy and SEM. The photographic documentation should follow a systematic approach [8,11,12,17,25,32] with (1) correct orientation of the entire broken part (occlusal surface on top), (2) labeling of the specimen regarding orientation (mesial, distal, buccal, palatal or lingual, (3) targeting zones of interest for detailed analysis and mapping the direction of crack propagation over the entire fractured part based on the correct identification of characteristic fracture surface features (wake hackle, twist hackle, arrest lines, compression curl and more) within these zones. It is important to give photographic evidence for such mapping. The origin should be thoroughly searched and at least a location identified from which the crack has started. If identified, than at least one higher magnification image of the origin is needed.

Clinical failures are often more complex than lab-scale failures, the latter being rather straightforward with regards to fractographic analysis. Unfortunately, due to an incomplete fractographic approach, some fractures of broken parts may be wrongly identified as an origin because the whole fracture surface was not properly analyzed in terms of direction of crack propagation (dcp). Hence, a secondary fracture event may be confused with a crack origin if only one picture is shown. Fig. 10a illustrates such a misleading documentation. It corresponds to a partial view of fractured zirconia abutment which was directly veneered for a premolar crown reconstruction and screwed onto a titanium implant. The fracture occurred after 2 years of intra-oral use. The shoulder part of the abutment shows a chip fracture (Fig. 10a) which looks like the origin (white arrow) but in fact this is only a secondary fracture event. This can be proven by the very fine hackle lines indicating the main crack direction, as pointed by the black arrows. Looking at a different image further up (Fig. 10b), the fracture origin is clearly situated at the internal angle (large black arrow), below the screw head. A large twist hackle is visible emanating out of that corner followed by many fine hackles indicating the dcp (Fig. 10c, 800×). Chip damage on that inner side of the corner can be observed in connection with

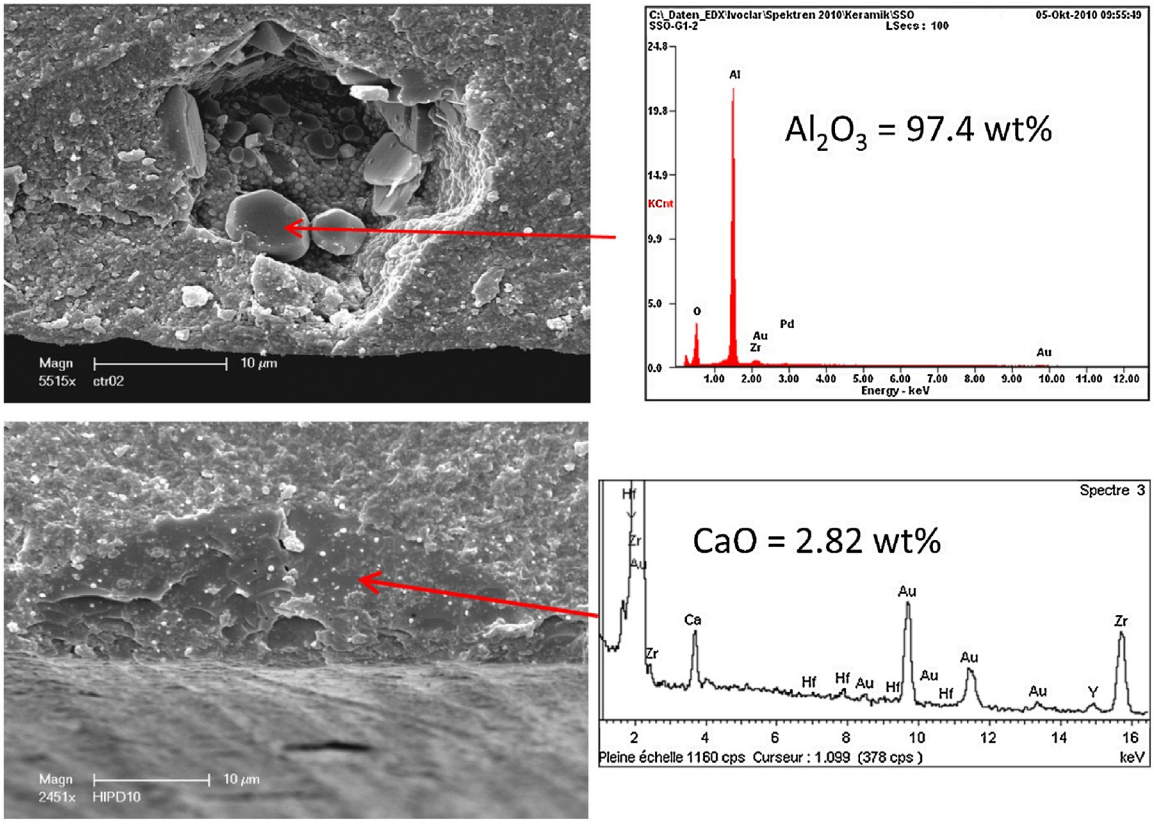

Fig. 9 – Failure origins in 3Y-TZP bend bars. EDX combined with SEM allows identification of contaminants composition. The top image shows alumina particles inside a pore within a critical flaw (a 20 × 30 μm) connected with the tensile surface. The bottom image shows a critical flaw of 14 μm in depth containing 2.82 wt% CaO responsible for grain growth.
Recommendation 3: When identified fracture origins show problems such as inclusions, second phase grains, contaminations or abnormal grain growth, a chemical spectral analysis should be performed within the critical flaw (Fig. 9) for feed-back in relation to processing issues. When possible, make use of the backscattering mode to better visualize the critical flaw (Fig. 8).

the crack origin. Reasonable speculation can be made that these damages were created during the screw tightening or screw contact while the crown is cyclic loaded during function. This case is further documented in Fig. 11 with the purpose of having an overall robust stereomicroscope documentation in which the various origins, dcp, and secondary chipping fractures are clearly indicated. These secondary events are visible on both mesial and distal shoulders as well as at the area of direct contact with the screw head. The chipping fracture at the screw head contact (slight metal traces visible on the inside) was arrested in the zirconia abutment. The black arrows show the overall dcp. The red arrows indicate multiple fracture origins at the corners. Fig. 11c,d shows both fractured parts joined together in which the crack pattern is visible as well as the missing chipped ceramic at the shoulder level (secondary event). When available, assembling matching parts is essential in fractography to better understand the fracture as it provides information about the overall crack pattern, crack bifurcation, crack branching, presence of cone cracking and missing parts. In clinical dentistry, this has been very efficiently applied to recovered all-ceramic crowns using only stereo microscopy [21,22] before adding SEM for more detailed views of the origins located at the crown margins [26]. A reference paper by Quinn et al. [11] has introduced this method to the dental community reassembling broken parts on three whole all-ceramic restorations and successfully describing the failure event, mapping the crack propagation along the fractured surfaces, and identifying the fracture origin. Usually the half showing a better view of the origin is published, but the other half should be also kept as a back-up to confirm the initial findings [15].

5.2. *Origin related to manufacturer processing*

Processing flaws from the manufacturer may be involved in the premature failure of a clinical component. The case presented in Fig. 12 is the same as in Figs. 10 and 11. On the rim connecting the simultaneous developing corner crack origins on both sides (see stereomicroscopy in Fig. 10), a close-up view (Fig. 12c,d) in the area of the central white rectangle shows multiple cracks. Possibly these were introduced during the pre-sintered state machining of the abutment part. This area involves a screw contact and is considered sensitive to damage [25,51]. The manufacturer should therefore have some means to facilitate crack detection in the green state before sintering and packaging the block for sale. Fluorescent penetrant liquids, water-washable and water-based (such as Ardrox® 920A, Chemetall), are used in the aeronautic industry and also for

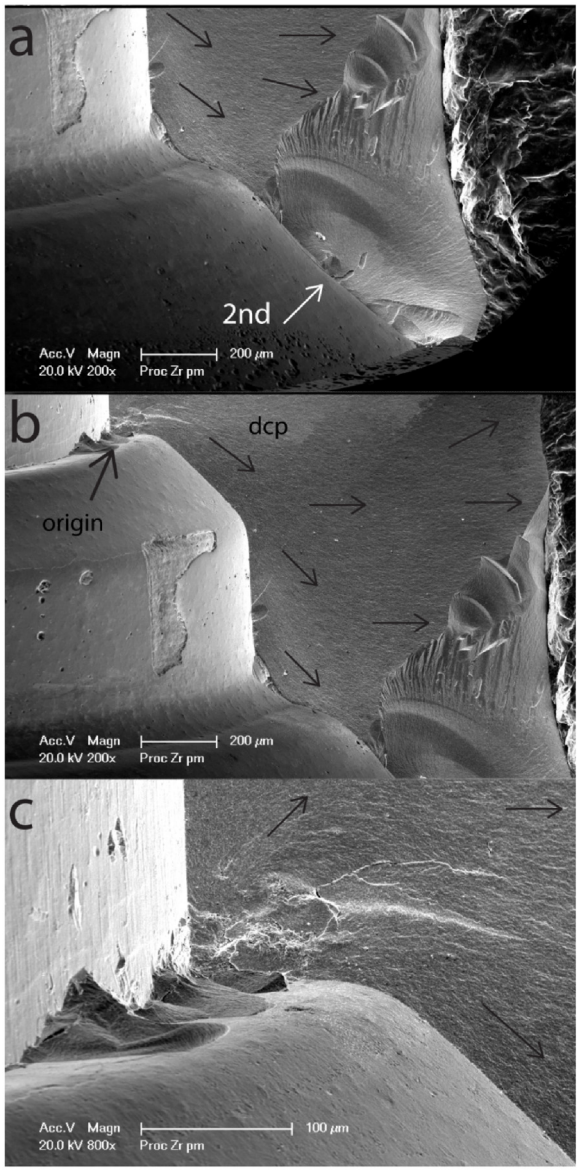

Fig. 10 – Fracture of a veneered zirconia abutment screwed onto a titanium implant. Fracture occurred after two years of intra-oral use. (a) shows a secondary chip fracture at the shoulder level which *should not be confused* with the fracture origin seen in (b) and (c). If only (a) is shown in a paper claiming this chip-fracture to be the origin of the critical fracture of the abutment-crown, then an erroneous message will be delivered. On the same image a more expert understanding of the fracture surface and its interpretation will recognize the presence of small hackle indicating the prime direction of crack propagation (dcp, black arrows). (b) and (c) show the correct origin of the critical crack located at the corner. A major twist hackle is emanating from it rotating outwards. Further fractographic documentation of this case is provided in Figs. 11 and 12.

zirconia to reveal cracks as the fluorescent liquid penetrates any crack and shines in a UV chamber. An example of such non-destructive quality control performed by manufacturers is shown in Fig. 13. These cracks cannot be repaired and this piece is to be discarded in order to avoid a useless sintering process and valuable working time loss. Other methods for crack detection have been evaluated for dental ceramics using light microscopy, SEM and fluorescence microscopy [52], the latter being the most efficient crack detecting method. Overall, more quality control should be performed both at the manufacturer and dental technician level when working with brittle materials in which microcracks can be introduced during the processing steps. Zirconia frameworks should all undergo at least a transillumination screening test after sintering (Fig. 14) before applying the veneering ceramic.

5.3. *Cracks related to laboratory processing*

5.3.1. *Presinter grinding damage*

Descriptive fractography can also be used for elucidating cracks in zirconia. Undetected cracking in the presintered state can occur and is often only visible after sintering using transillumination. Due to the translucent nature of dental ceramics a lateral illumination with a light source combined with a stereomicroscope helps detecting the presence of cracks in the bulk of a restoration. At this stage, the cracked part cannot be clinically used anymore but it can serve the purpose for determining when the crack was introduced (i.e., pre- or post-sinter). An example of such a fractographic case analysis using a systematic approach is given in Fig. 14, showing a crack running from the margin up along the side wall and through the thickness of a zirconia framework using transillumination. Traces of grinding tools are visible at the margins. As with the *in-vitro* bend bars, a close-up examination of the fracture surface under the SEM will indicate the direction of the crack propagation on the open fracture surface as well as the shape of the grains. When free-air sintering occurs, the grains have a round shape as opposed to angulated when fractured after sintering. Pre-sinter cracks can occur from the CAD–CAM machining tool in the green state or from reshaping with burs by the dental technician. In order to analyze the fractured surface under the SEM, the cracked area will be cut off a few millimeters away on each side of the crack and separated at the bottom of the crack. The two halves are then labeled (part #1 and part #2) and further analyzed under SEM (Fig. 15).

Both parts are seen in Fig. 15 showing the grinding marks on the outer surface near the margin (Fig. 15a). A higher magnification (Fig. 15b, 12,000×) of the grains on that surface (black rectangle) reveal that they are round, which means unconstrained free air sintering. Confirmation is provided with part #2 in which the compression curl is clearly visible on the inner side (Fig. 15c), confirming that the direction of crack propagation (dcp) moved from the outer surface of the framework (where the grinding marks are) towards the intaglio surface. A higher magnification in Fig. 15d (50,000×) shows quite rounded grains from unconstrained sintering due to a crack introduced during green state grinding.

Another example of grinding cracks is shown in Fig. 16, a clinical failure of a zirconia 4-unit bridge after 9 months of intra-oral use. In this instance the embrasure region between

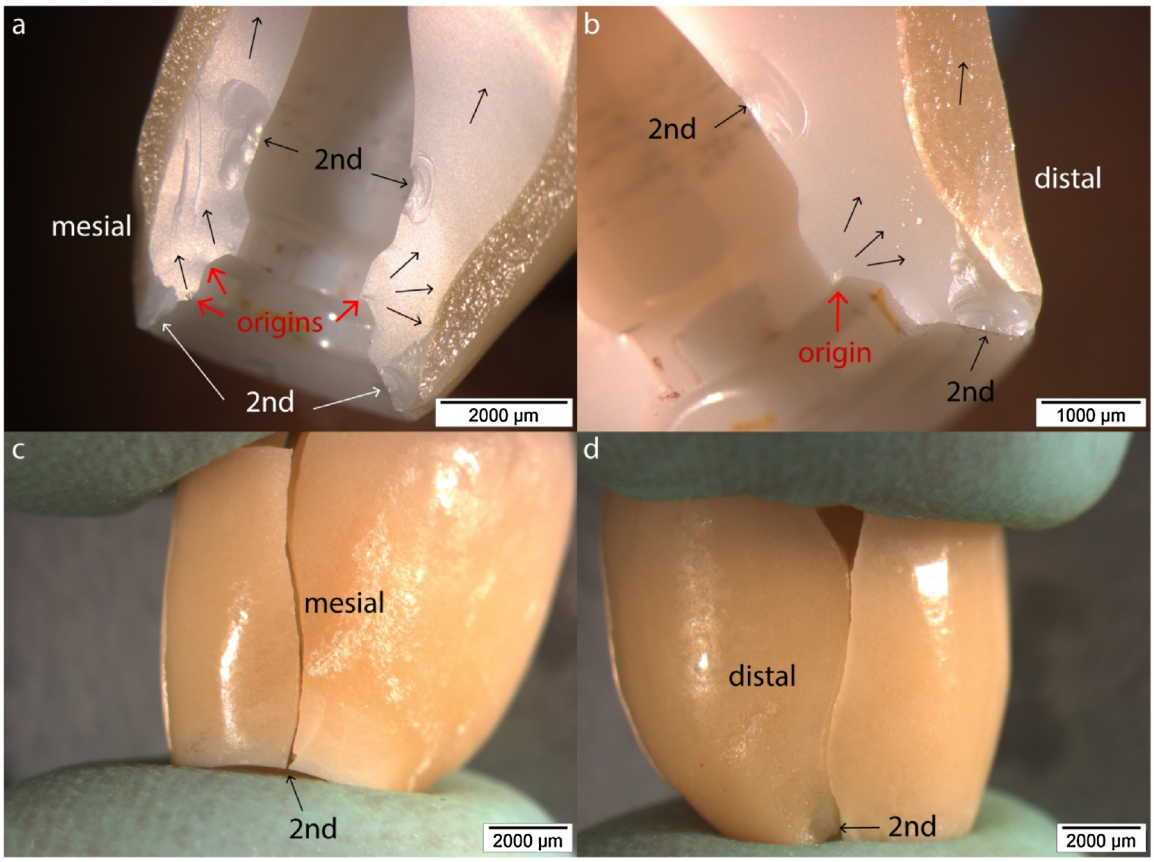

Fig. 11 – Procera zirconia abutment directly veneered for crown restoration screwed onto a Titanium implant. Fracture occurred after 2.5 years in-situ. Matching halves are joined together with some material loss visible at both margins (mesial and distal). Failure origins are marked with red arrows. The crack propagation direction is marked with black arrows. Secondary events (2nd) are visible at the margins (loss of material) as well as at the level of the screw head contact showing starter cracks from the inside towards the outside on both sides but confined to the zirconia framework (more failure analysis of this case in Fig. 12) (For interpretation of the references to color in this figure legend, the reader is referred to the web version of this article.)

Recommendation 4: Clinical failures should be documented using a systematic approach [12]. An overall view image is needed showing the mapping of the crack propagation direction supported by higher magnifications of key fractographic features. The origin should be carefully identified. Reassembling broken parts should be performed every time matching pieces are available.

the premolar pontic and the molar abutment crown was reshaped by the dental technician, most certainly to create sufficient space for the papilla. The purpose here is to show the grinding damage in the presintered state at the embrasure region. How do we reach this conclusion without looking at the shape of grains? The answer is given by zooming in with the SEM at that site. A preliminary search for hackle lines moving from the bottom to the top (not shown here) made us focus on the embrasure region (Fig. 16a,b). A closer view (Fig. 16c, 1500×) of the embrasure shows tool marks (little steps) from bur adjustment as well as cracks. Further zooming in with the SEM at 5000× magnification (Fig. 16d) shows horizontally running cracks over 100 µm distance in between the grinding mark. Failure of the cracks to fuse during the sintering process is an indication that the cracks were introduced in the presintered state during framework reshaping by the dental technician possibly to create more space for the papilla.

5.3.2. *Failure from interfaces*

Issues related to multilayer interfaces is extensively addressed in a separate ADM guidance document [53]. Descriptive fractography is essential for assessing the correct failure cause, especially when interfaces are involved. The laboratory layering technique over a zirconia framework can unfortunately introduce many stress related problems due to CTE differences, irregular veneering ceramic thicknesses, contaminations, poor wetting or air entrapping. Temperature gradients exist throughout the veneering ceramic over the zirconia core as well as thermal residual stresses which are accentuated near the interface when fast cooling is performed [54–68]. Such residual stresses close to the interface are often considered as major contributors to premature veneering ceramic chip-fractures. If in addition, defects such as trapped air pockets (i.e., bubbles) are incorporated during the layering technique at the interface where thermal residual stresses are concentrated, premature fracture will occur as shown in a

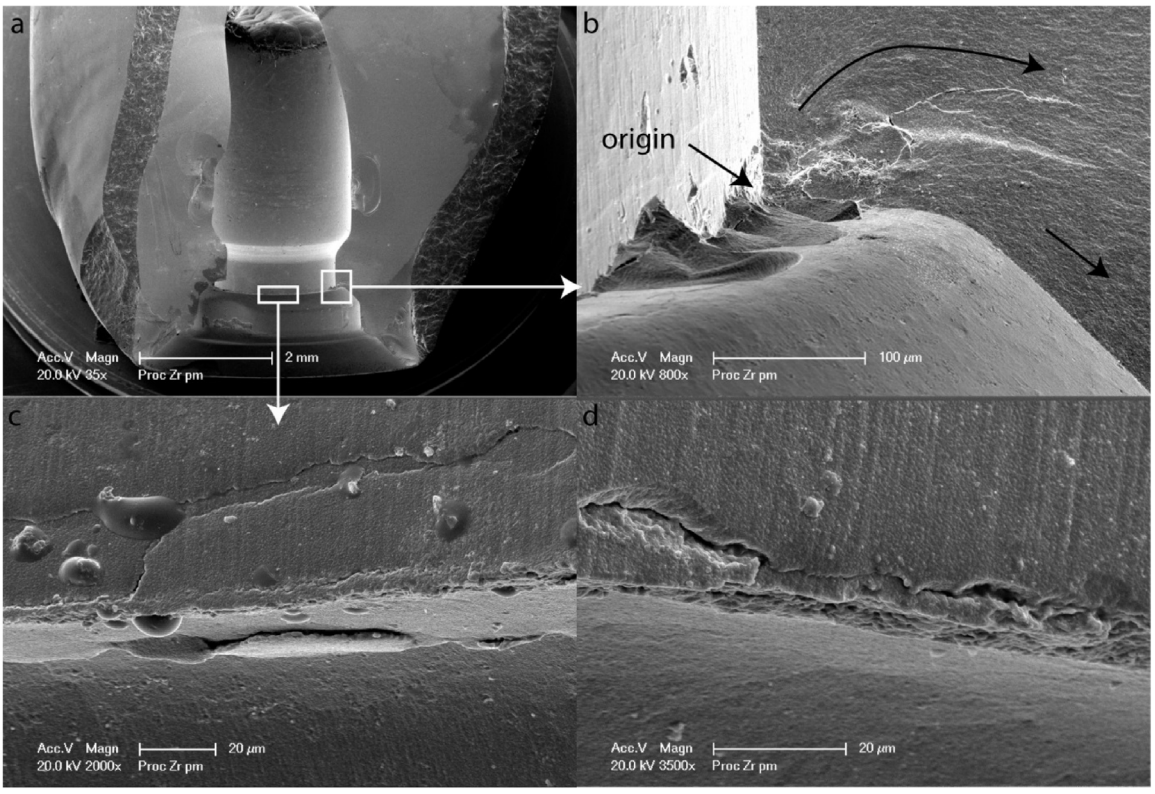

Fig. 12 – Same case as described in Figs. 10 and 11. Further SEM analysis of the inner rim show evidence of major precracks spread over the entire length of the rim, thus weakening the structure. These cracks are related to manufacturer processing problems.

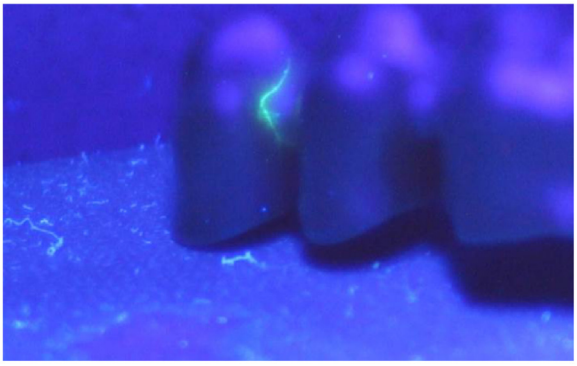

Fig. 13 – Zirconia green body framework dipped in Ardrox® 920A, a water-washable and water-based fluorescence liquid, revealing a crack in a UV chamber (image courtesy of Diadem, F).

Recommendation 5: When zirconia fractured parts are available such as abutments, implant or, bridge frameworks involving connectors, one should search for additional processing issues such as sintering problems, compaction, and presintered state grinding induced cracks.

clinical case in Fig. 17. This implant supported central incisor crown, consisting of a 3Y-TZP core and a fluorapatite veneering ceramic, fractured after 2 months of intra-oral use. The fractographic findings point back to a fracture origin being an important (0.6×1 mm) central void between the veneering ceramic and a liner layer over the zirconia core. The crack started from the edge of the pore at the red arrows, radiating outwards and propagating along the white and black arrows with a twist around the pore as confirmed by the presence of fracture surface features (i.e., hackle, wake hackle, twist hackle, arrest lines). The central pore comes from the layering technique entrapping some air and creating a stress state around the pore [54,57]. Thermal residual stresses may have contributed to this early failure even though the dental technician used a compatible veneering ceramic (e.max Ceram, coefficient of thermal expansion CTE = $9.5\,10^{-6}/^{\circ}$K) and slow cooling. Thermal stress gradients remain distributed within the veneering ceramic but their magnitude and distribution is complex as so many parameters play a role (ΔCTE, firing parameters, veneering ceramic thickness, core-veneering ceramic thickness ratio, zirconia-veneering ceramic interface). In this case, the thickness of the veneering ceramic was quite important ($\geq$2 mm). From experimental data, it is known that increasing the thickness ratio of the veneering ceramic to the zirconia core will increase the development of residual tensile stresses [55–58]. Interestingly – in contrast to common believe among dentists – the chipping event occurred completely in the veneering layer without touching the interface. In most fractographic studies, a thin remaining veneer layer was detected on the zirconia interface. This layer presents evidence of residual stresses close to the interface [67–69]. From a clinician's perspective the fracture plane appears whitish

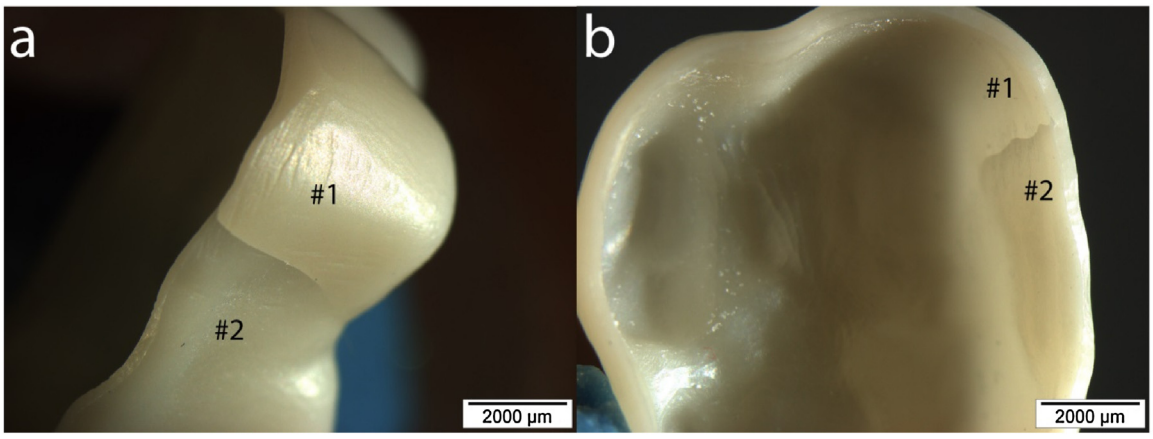

Fig. 14 – Crack visible through transillumination on a sintered zirconia crown framework. View from the outside (a) shows a crack from the margin up along the side wall as well as through the thickness as visible from the inside (b). Note grinding marks near the margins.

and the conclusions are drawn too quickly. The reader may also consult a clinical veneering ceramic failure case involving thermal residual stresses and fully documented with fractography and EDX analysis [16].

5.4. *Origin related to contact wear*

Contact wear from chewing is a physiological event. The amount of wear will greatly vary among individuals as it will

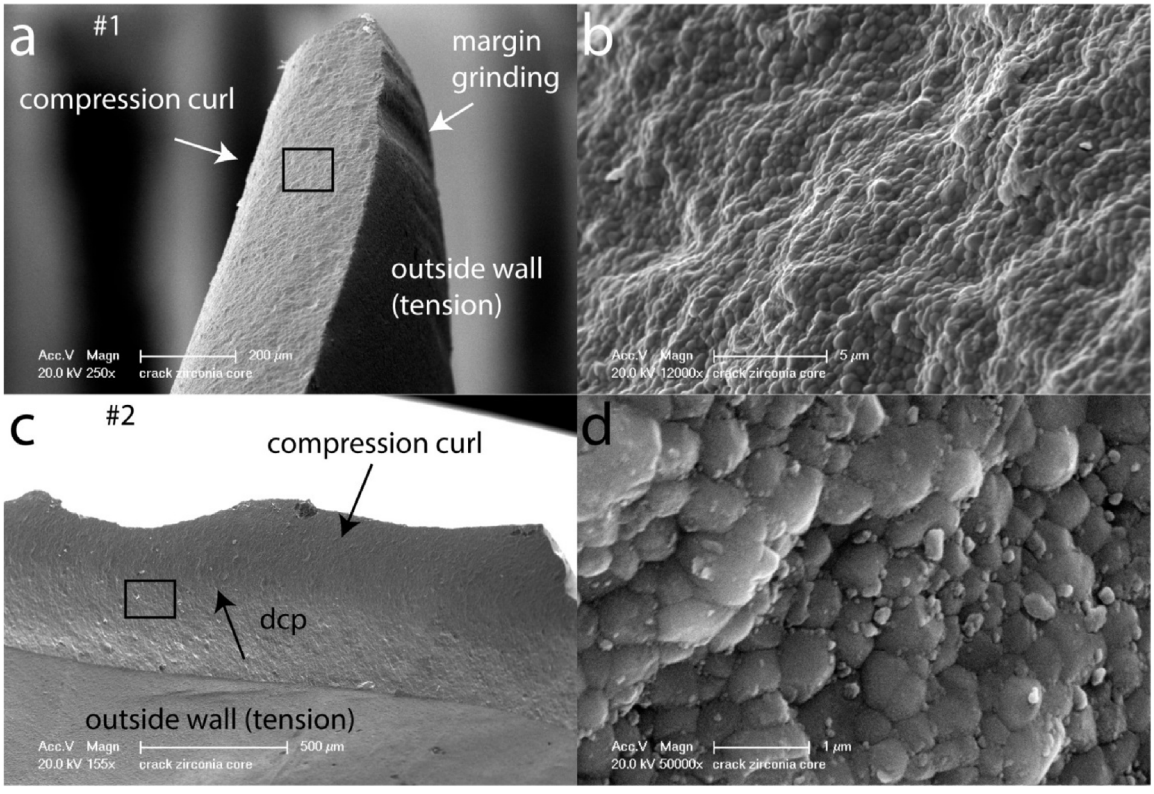

Fig. 15 – SEM fracture surfaces of both matching sides (#1, #2) of the crack in the zirconia framework illustrated in Fig. 13. Grinding marks are visible on the outer surface near the margin (a). At higher magnification (12,000×) the grains on that surface (black rectangle) can be seen to be round in shape, which means free air sintering (b). Confirmation is provided with part #2 in which the compression curl is clearly visible on the inner side (c) confirming the direction of crack propagation (dcp) moving from the outer surface of the framework (were the grinding marks are) towards the intaglio surface. A higher magnification in (d) (50,000×) shows quite round grains from free air sintering due to a crack introduced during green state grinding.

Recommendation 6: Pre- or post-sinter cracking in zirconia can be determined by looking at the grain morphologies.

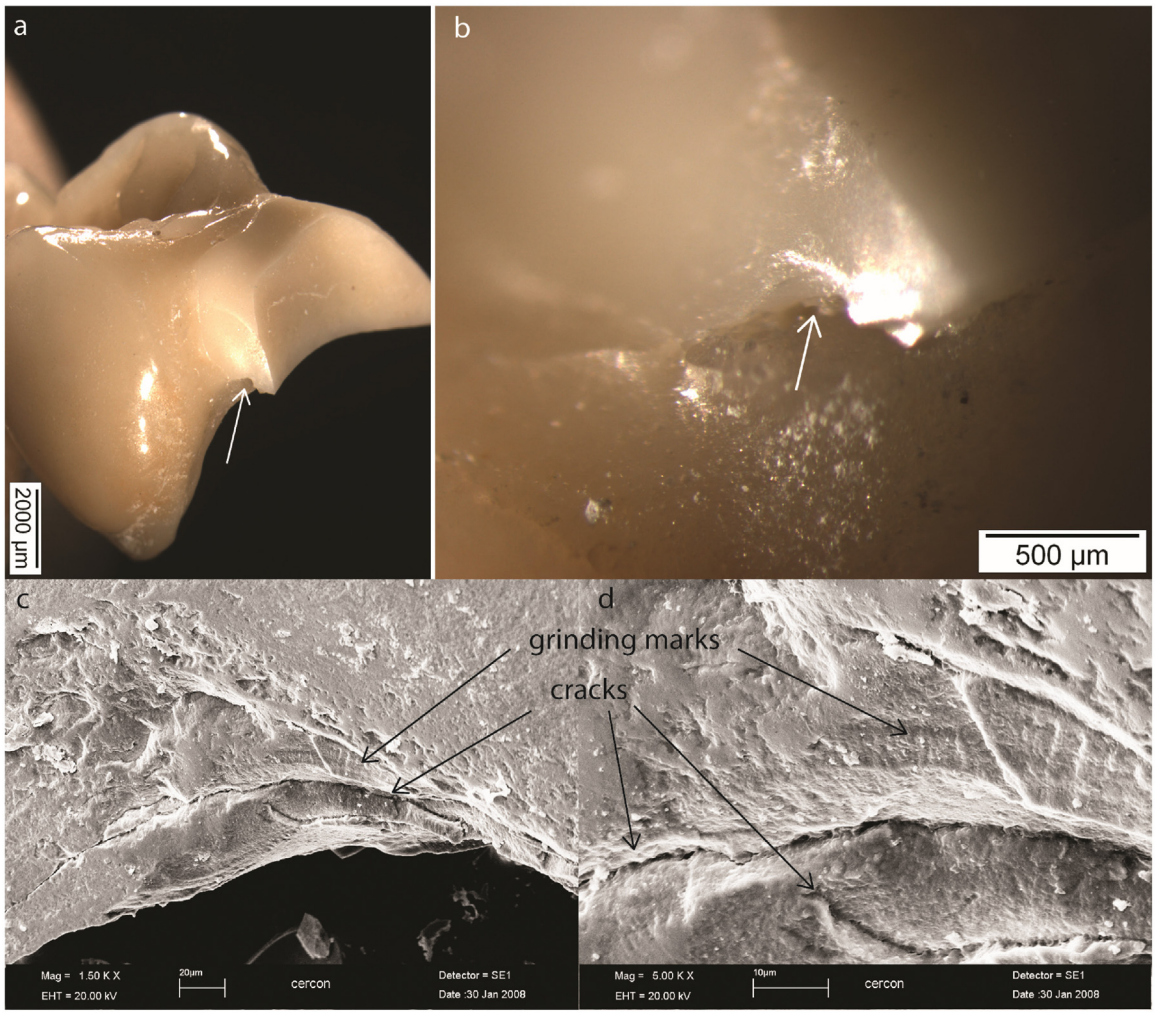

Fig. 16 – Clinical fracture of a zirconia 4-unit bridge after 9 months of intra-oral use occurred between the premolar pontic and the molar crown abutment. The embrasure region is marked with a white arrow. Higher magnifications (c,d) show grinding marks from a bur as well as cracks. The partial fusion of these cracks indicates that cracking occurred in the presintered state.

depend on the coupling materials involved (ceramic, enamel, resin composites, metal alloys), the contact loads, contact surface, direction of loading and the surface roughness. The mechanical properties such as hardness and fracture toughness of the ceramic, subsurface residual stress state, the contact pressure and its frequency, will dictate the surface degradation over time. Ceramic chipping is classically related to contact wear as most origins will show a worn contact surface. When possible, information regarding the opposing dentition (restorative material, wear facets, occlusion) should be collected. An example of a fractographic documentation of a contact wear related veneering ceramic fracture is illustrated in Fig. 18, an in-situ tooth-supported zirconia veneered crown chip-fracture. The emphasis here is to show the importance to document properly the occlusal surface which is strongly associated with the fracture event. Fig. 18a provides an overall image of both the occlusal surface and the fracture surface. The black arrow points to the origin of the chip-fracture. The white arrows indicate the dcp. Further magnifications focus on the fracture origin (Fig. 18b) and the important contact wear (Fig. 18c,d) involved in the fracture process (brittle fracture mode) of a non-leucite veneering ceramic (Zirox, Wieland). In fact, under repetitive contact wear it becomes difficult to identify a single origin of failure. Contrary to in-vitro fractography, clinical wear origins are mostly a result of repetitive degradation over time, exhibiting larger surface damage zones instead of a single fracture origin. Fig. 18b shows a severe damage accumulation zone, being responsible for the fracture event. Only the actual fractographic patterns on the fracture plane can be traced back to the region of the origin [70].

5.5. *Fractographic "friendly" and "unfriendly" ceramics*

The identification of fracture surface markings is highly dependent on the microstructure of the ceramic and the processing (i.e., handlayering, heat-pressed ceramics, sintered

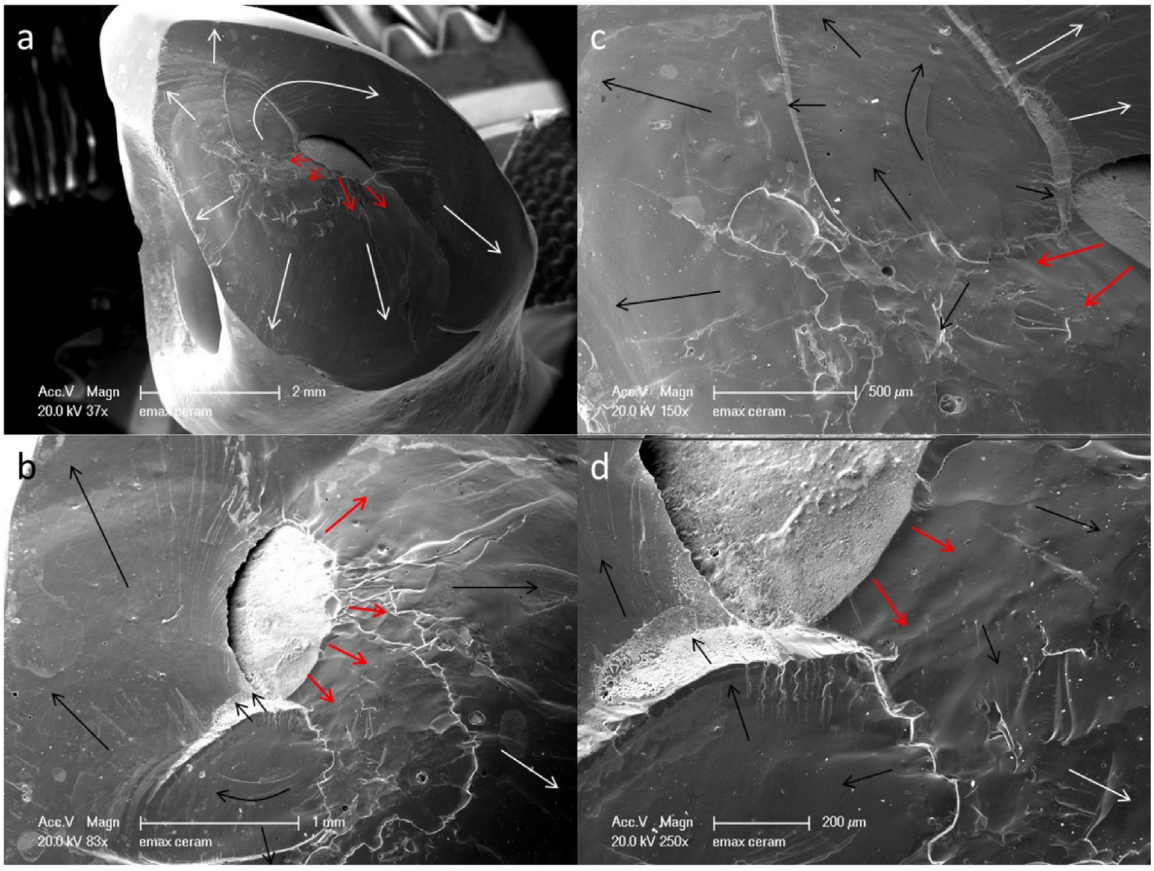

Fig. 17 – SEM images of a veneering ceramic fracture after two months involving the zirconia core interface. A void of approximately 1 × 0.5 mm over the zirconia framework covered by a ceramic liner layer was the origin of the crack. The crack started at the red arrows radiating outwards, propagating along the white or black arrows with a twist around the pore as confirmed by the presence of fracture surface features (i.e., hackle, wake hackle, twist hackle, arrest lines). Thermal residual stress may have contributed to this early failure. (For interpretation of the references to color in this figure legend, the reader is referred to the web version of this article.)

Recommendation 7: Failures involving an interface should be very carefully analysed by fractography. The probability is high that thermal residual stresses, increased ratio of veneering ceramic to zirconia core and irregular veneering ceramic thicknesses have contributed to the fracture event. Therefore, when possible, information on sintering schedules, cooling rates and CTE of the veneering ceramic should be gathered from the dental laboratory.

CAD–CAM ceramic blanks). Some are very easy to analyze such as veneering ceramics over zirconia because the crystalline content is very low or absent and the appearance is like a glass as opposed to others that are more complex such as lithium disilicate, feldspar-based ceramics or alumina. It is all a matter of microstructure, fracture surface roughness, presence of tiny pores showing wake hackle, magnification and time spent using both the stereomicroscope with lateral illumination and SEM to analyze the fracture surface. An example of an unfriendly microstructure is shown in Fig. 19 for a feldspar-based CAD–CAM ceramic (Vita Mark II) (Fig. 19a) as well as lithium disilicate glass-ceramics (Fig. 19b). The feldspar-based ceramic shown has a rather rough fracture surface microstructure and the presence of a few pores may give some localized hints as to the direction of crack propagation (dcp). A careful analysis of the entire piece is therefore needed to see larger features such as a compression curl or arrest lines over the entire part. The lithium disilicate has a smoother fracture surface compared to the feldspar-based ceramic but has a very dense structure and usually there are little to no pores to rely on for the dcp identification. In the image in Fig. 19b a careful observation in the SEM allows one to distinguish many hackle lines running parallel to each other over the entire cracked surface. In such cases it is even more important to spend time with the stereomicroscope and use lateral illumination to bring out crack features at low magnification before going to the SEM. This is particularly true for lithium disilicate glass ceramics. An example of how a slight change of light angulation in the stereomicroscope can highlight key crack features such as hackle, wake hackle, Wallner lines is shown in Fig. 20. A lithium disilicate crown broke during a try-in over a titanium abutment. The inner occlusal corner was the crack origin at

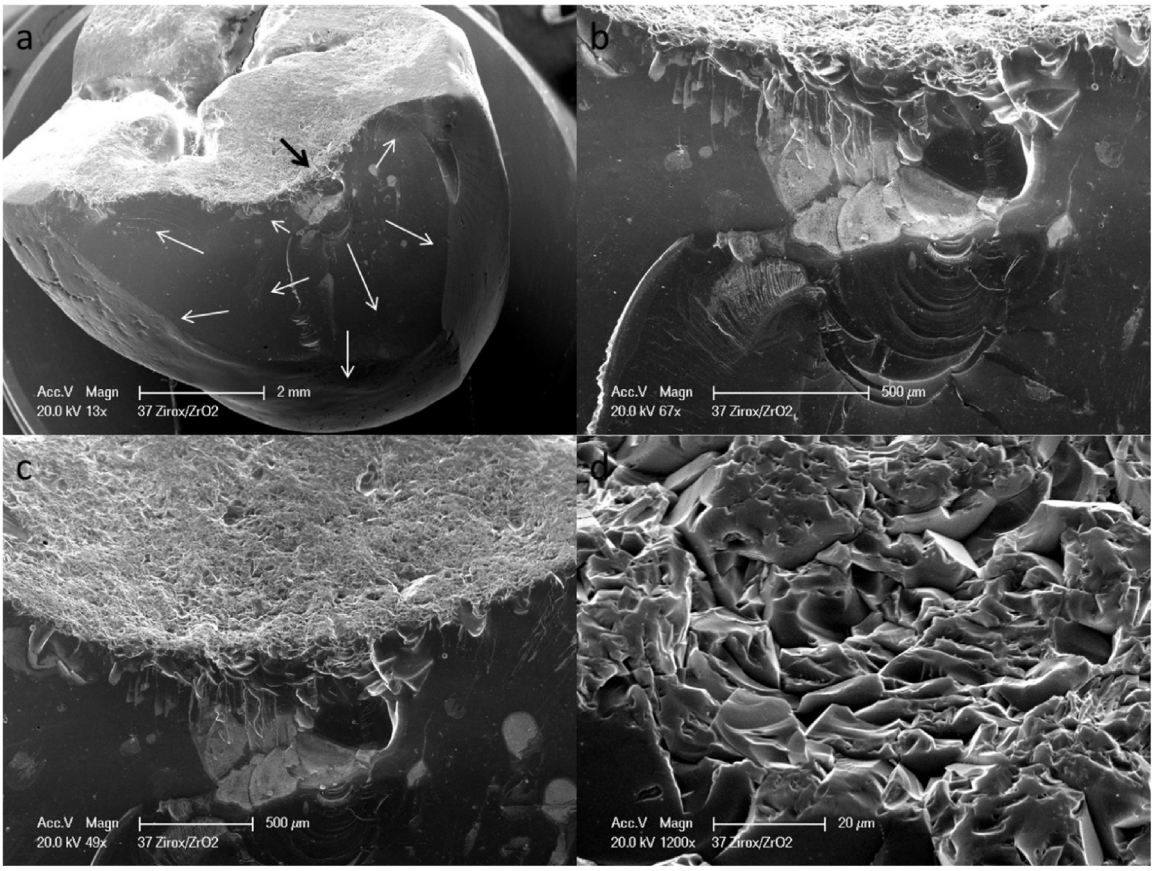

Fig. 18 – Replica fractographic analysis of a 12 months chip-fracture of a non-leucite veneering ceramic (Zirox) over a zirconia core. (a) Provides an overall image of both the occlusal surface and the fracture surface. The black arrow points to the origin of the chip-fracture. The white arrows indicate the dcp. Further magnifications focus on the fracture origin (b) and the substantial worn occlusal surface (brittle fracture) (c,d) involved in the fracture process.
Recommendation 8: When chip fractures are involved, the occlusal surface has to be scrutinized and searched for localized contact wear in the vicinity of the fracture origin. Especially in wear related fractography, the antagonist dentition provides additional information (i.e. material in contact, wear facet, occlusal contacts)

it was rocking over the abutments sharp rim inducing a localized contact pressure which was unfortunately combined with some ceramic roughened surface from diamond bur adjustments by the dental technician to provide some space in this area. Fig. 20a shows a stereo image in which the illumination is not adequate as no crack features are visible. By changing the light incidence angle the fracture surface starts to become visible with many crack features such as hackle, wake hackle and Wallner lines (Fig. 20b). The higher magnification of the crack origin (Fig. 20c) has just the right lightening to reveal several hackle departing from the inner corner. When dealing with alumina (Fig. 21a) or zirconia cores (Fig. 21b) covered with their respective veneering ceramic, a very careful study of the interface will be most helpful in determining the dcp as again, the layering technique will incorporate some pores which may give rise to some wake hackle and twist hackle The very low content of leucite crystals in the veneering ceramic applied over both zirconia and alumina makes them easy materials to analyze.

6. Fractography from replicas

Replication of a fracture surface with silicone impression material [14] has the purpose of securing valuable information regarding the fracture surface of a broken restoration that is still *in situ* and which may not be retrieved without damage. Typically it would be a remaining crown portion for which the detached broken part has been lost [14]. The critical issue is to obtain a good replication of the entire left over part which includes the fracture surface for crack features, the occlusal surface for a search of contact damage, as well as the crown contours in order to be able to orient and locate the fracture event with respect to the crown anatomy. Although taking an impression is not difficult, some guidance should be followed in order to obtain a replica of good quality. The first issue is to have a fractured surface *in situ* that is as clean as possible prior to impression taking. For that, a combination of water spray and air should be abundantly blown on the fractured

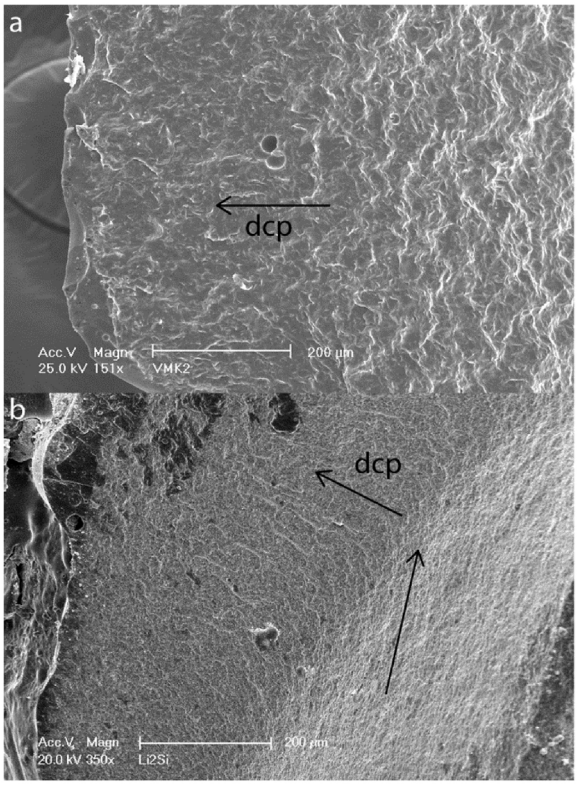

Fig. 19 – A fractured surface of a feldspar-based ceramic (Vita Mark II) (a) and of a lithium disilicate glass-ceramic (b) is shown. Both are considered as rather difficult for identification of fractographic surface crack features and determination of the direction of crack propagation (dcp).

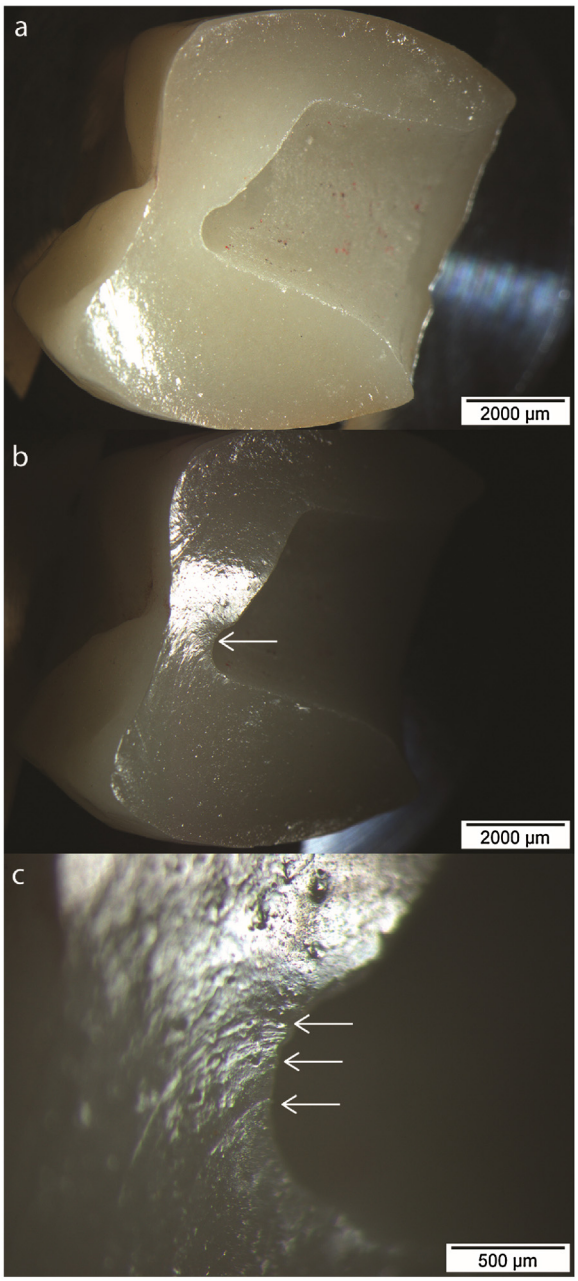

Fig. 20 – A lithium disilicate try-in failure is documented using a stereomicroscope and lateral illumination. In (a) no fractographic features are visible in the overall image. By changing slightly the angle of light incidence it is possible to make key features to appear very clearly as seen in images (b) and (c). The white arrows indicate the crack origin failure at the inner occlusal corner.

surface to get rid of a maximum of loose plaque and biofilm. Additional cleaning should be obtained by carefully rubbing the surface with a chlorhexidine or NaOCl 2% soaked foam polymeric pellet avoiding any metal contact on the fractured surface. As a matter of fact, no metal explorer nor cleaning or polishing pastes should be used as these will permanently scratch the fractured surface masking in part the tiny fracture surface features that the fractographic analysis is trying to identify. The impression material for the replica should be an addition crosslinked silicone such as a polyvinylsiloxane (PVS) and not a polyether because of chemical incompatibility with the epoxy pouring material. Fig. 22 shows an example of a clinical fracture surface of a zirconia veneered bridge with delamination of a portion of the veneering ceramic (Fig. 22a) as well as a polyether replica poured with epoxy (Fig. 22b) both viewed under the SEM in the same area. The polyether shows a poor surface reproduction of details due to its chemical incompatibility with the epoxy.

Ideally two replicas should be taken *in situ* as the first one may have some adherent plaque on it masking important details whereas the second impression performed on a cleaner surface will secure more surface details. Preferably an ultralight bodied impression material should be used as the wetting and detail reproduction of the fractured surface will be better. An example of such detail reproduction based on the viscosity of the impression materials (ultralight versus light body) is illustrated for a zirconia bend bar fracture surface. Fig. 23 shows the original fractured zirconia surface, Fig. 23b is the epoxy reproduction of an ultralight body PVS (Express 2, 3 M) replica, Fig. 23c of a light body PVS (Express 2, 3 M). The degree of detail with the light body PVS impression materials is not as good as with the ultralight body. Some silicone impression materials will however degas as a reaction of Hydrogen release from the silicon and are therefore not suit-

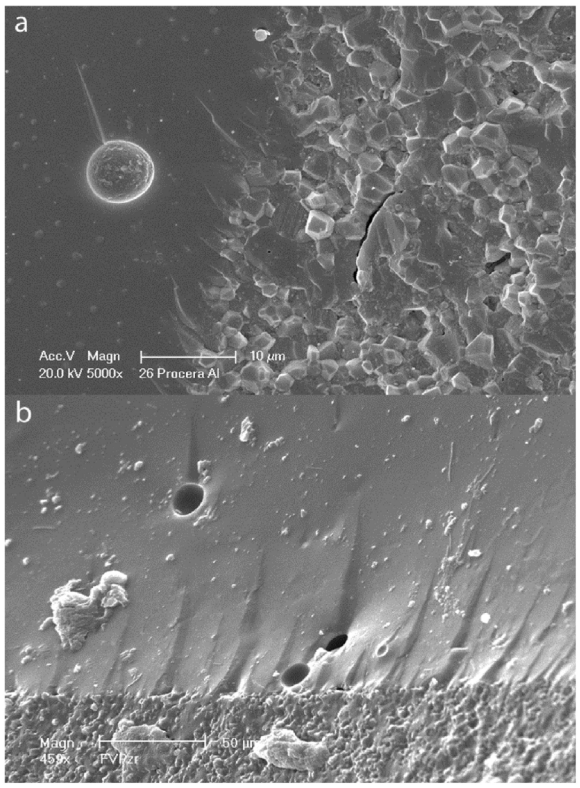

Fig. 21 – Alumina core (a) and zirconia core (b) with their respective veneering ceramics. The veneering ceramic in both cases show easy recognizable features such as wake hackle, hackle and twist hackle visible at the interface as a continuation of the crack front moving from the core materials towards the veneering ceramic.
Recommendation 9: Be aware of the microstructural differences of ceramics which will render the fractographic analysis more or less complex. If a glassy veneering ceramic is present it will greatly help visualize fractographic features. Use lateral illumination (grazing angle) in a stereomicroscope to visualize (bring out) features with ceramics that are more complex (i.e., Lithium disilicate, feldspathic porcelain).

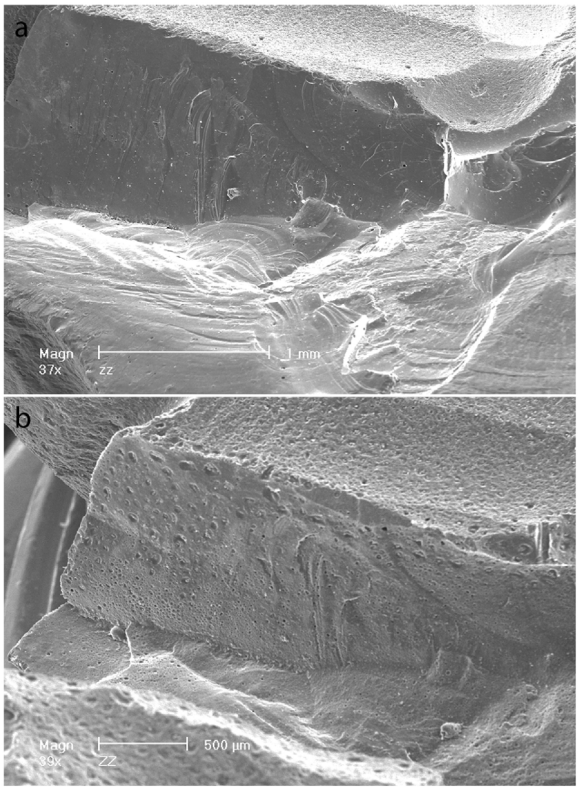

Fig. 22 – SEM images of a clinical fracture surface of a zirconia veneered bridge with delamination of a portion of the veneering ceramic (a) as well as of a polyether replica poured with epoxy (b) both viewed in the same area. The polyether shows a poor surface reproduction of details due to its chemical incompatibility with the epoxy.

able for fractographic analysis as many air bubbles will appear on the epoxy-poured replica as shown in Fig. 23d (Aquasil PVS, Dentsply).

7. Cleaning procedure

The cleaning of *in-vivo* specimens is of key importance for eliminating deposits of adherent plaque or biofilms (mainly bacteria colonization) on the fractured surface due to exposure to the oral environment. Such biofilms cannot be easily removed if one uses only water spray, cotton swabs to rub it off or ethanol solutions and ultrasound. A chemical dissolution has to be carried out without interfering with the ceramic composition. Most of the existing standards are quite general with regard to their cleaning recommendations and mention both ethanol and acetone for ceramic surface cleaning, which is adequate for in vitro specimens. What has however proven to be efficient regarding biofilms on ceramic is a 16% solution of sodium hypochlorite (NaOCl) for 5 to 10 min in an ultrasonic bath. A SEM example is provided in Fig. 24a of a fluorapatite veneering ceramic fracture of an implant screw-retained all-ceramic crown which was retrieved a few days after fracture. The dental plaque had time to grow and to adhere to the fracture surface and was not dissolved after 5 min ultrasonic cleaning in a 100% ethanol solution (top image). SEM gold and platinum coatings can be removed by soaking the ceramic specimen for one minute in aqua regia (1 part by volume of HNO_3 + 3 part by volume of HCl) [8] but adequate precautions must be taken with this hazardous product (use of gloves, mask and eye protection). Aqua regia should not to be used on high-noble metal-ceramic restorations as it would attack the metal. Once the gold coating efficiently dissolved, the specimen was ultrasonically cleaned for 5 min in 16% NaOCl which dissolves the biofilm. After gold-coating again, the specimen was analyzed in the SEM. All key fractographic features such as hackle, wake hackle, arrest lines are now easily seen (Fig. 24b) as well as the area of palatal contact wear from which the fracture started.

As a rule, one has to secure the original state of delivery of the broken parts with a few stereo images before any major cleaning is performed. Collecting images on staining, cement

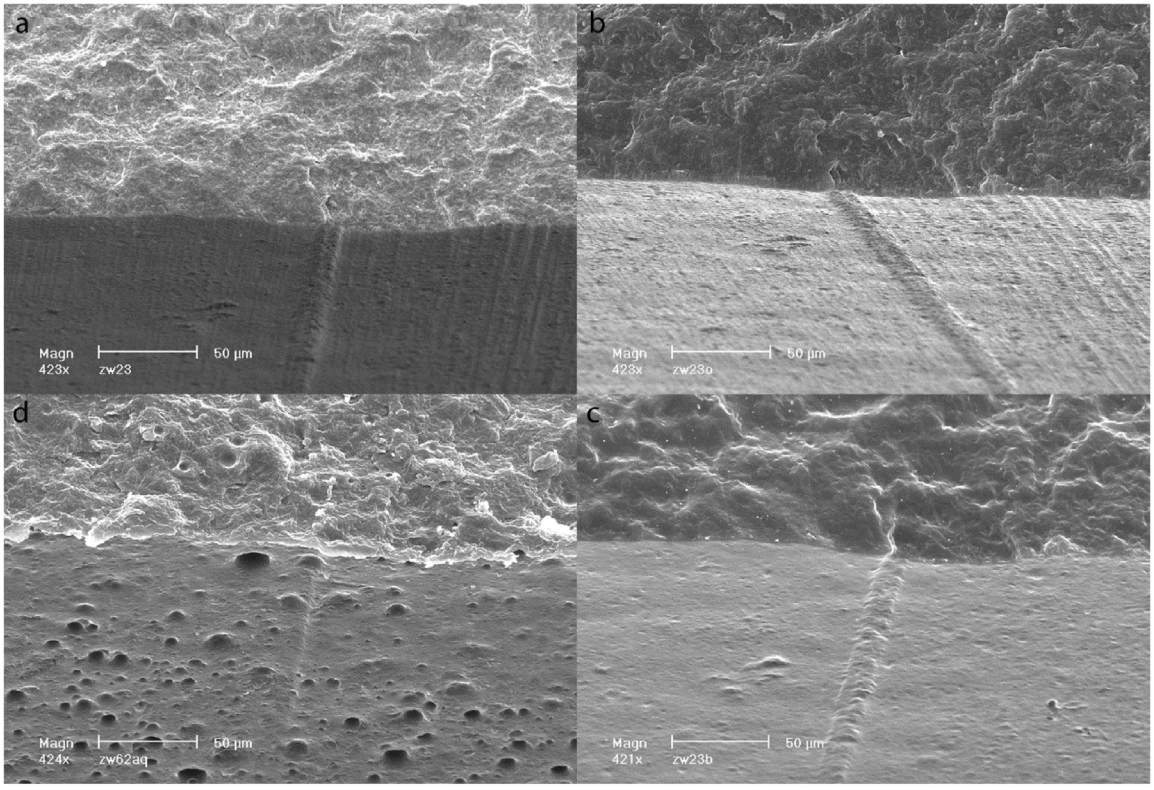

Fig. 23 – Illustration of a detail reproduction from an original zirconia broken surface (a) and an ultralight body PVS (Express 2, 3 M) (b), a light body PVS (Express 2, 3 M) (c). Hydrogen release is shown in (d), after pouring epoxy in a light body PVS (Aquasil, Dentsply).

Recommendation 10: Optimum reproduction of detail is obtained when using replicas with a very low viscosity such as an ultralight body silicone impression material. Tests of pouring epoxy and checking the degree of Hydrogen release (degassing) should be carried out before deciding which silicone impression material to use.

microleakage or surface scratching with metal instruments are part of the full case documentation [12].

8. Conclusion

Fractography is an extremely powerful and useful tool for failure analysis, whether applied to in vivo or in vitro fractured parts. Both quantitative and qualitative fractography have their place within Dentistry. Fractographic analysis should therefore always accompany fracture mechanics investigations, including strength, fracture toughness, wear and fatigue studies as well as every clinical trial in which failure is reported. This review guidance document should encourage and help all researchers who deal with fractured specimens to include systematically this powerful tool of failure analysis in their research work. The implementation of a more accurate use of fractography in every research paper should help avoiding incorrect statements as to the cause of failure. Clinical trials are encouraged to include fractographic analysis based on retrieved parts or on replicas as valuable information can be collected and appropriate feed-back delivered to the manufacturer, the laboratory and the clinician. Only with a global and united effort regarding failure analysis can we improve processing and design, develop new materials and deliver clinical recommendations on preventive measures and selection of appropriate restorative materials to avoid premature fracture.

Appendix A. A Systematic approach of data collection (adapted from the instructions given during the fractography course:) www.fractography.org

Description of material and failure event

1. Which ceramic (core/veneer) (maximum information from the processing of the dental laboratory would be helpful on how the ceramic was handled).
2. Intra-oral location (FDI tooth numbering).
3. Time in function (years or months, date of insertion, date of recovery).
4. Fracture event description by patient (typical questions: was the part mobile for some time, was the fracture sudden during chewing soft or hard food).

Collection of clinical evidence

1. In case you receive the broken part from the patient, do not clean it other than rinsing it quickly in chlorhexidine

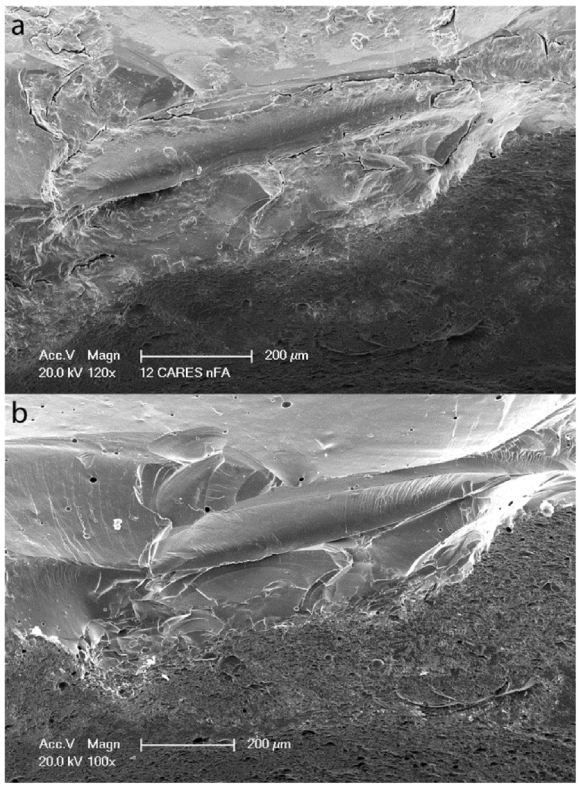

Fig. 24 – Illustration of a fluorapatite veneering ceramic chip-fracture of a zirconia screw-retained and implant supported single crown. The retrieval occurred a few days after fracture occurred, therefore covered with a thin biofilm. (a) shows the fractured surface after 5 min ultrasonic cleaning in alcohol. Most of the fracture surface features are masked. (b) (100×) shows the same clinical ceramic specimen after 1 min of aqua regia soaking to dissolve the gold coating followed with a 5 min ultrasonic cleaning in 16% NaOCl. The biofilm has been efficiently dissolved and the fracture origin next to a worn occlusal surface is clearly visible.
Recommendation 11: Clinical retrieved specimens should be ultrasonically cleaned in 16% NaOCl to dissolve the biofilm on the ceramic fracture surface.

as this part will undergo stereomicroscope documentation first.
2. Intra-oral photo of the remaining fractured part (helps orientation, location). X-Ray when dealing with broken implants or abutments as it provides information on bending moments and bone level.
3. A drawing on paper of the broken restoration may also replace an intra-oral photo.
4. Take a replica (preferably two in a row) of the fractured part remaining *in-situ*. First clean the surface with a cotton pellet soaked in Chlohexidine or NaOCl, then rinse thoroughly with water-spray before blow-dry. No metallic instruments nor cleaning pastes should be used on the fracture surface. Avoid any air bubbles within the replica on the fracture surface.
5. Recovery of the remnant part in-situ. Section 5 mm away from the fracture surface in case of a crown and try to dislodge it.

Documentation and analysis of a recovered failed part

1. Make macroscopic photos of the entire recovered broken part (helps orientation).
2. Clean the part (ultrasonic NaOCl 16% 5–10 min).
3. Conduct a systematic stereo microscope documentation of the fractured surface mapping all recognizable fracture features (compression curl, arrest lines, hackle, wake hackle (the latter one is visible at high 100–200× magnification only)).
4. Draw a sketch of the stereo findings. Use arrows to show the direction of crack propagation.
5. Do a SEM analysis confirming findings from stereo observations. Go through a systematic search of fractographic features which will allow a final mapping of the general crack path and sequence of events.
6. Create a powerpoint presentation including all pertinent clinical, stereo and SEM images in a structured way for discussion with colleagues. Remain clear, precise and concise!

REFERENCES

[1] ASTM-C1322-15. Standard practice for fractography and characterization of fracture origins in advanced ceramics. ASTM International; 2015.
[2] EN-843-6:2009-12. Advanced technical ceramics – mechanical properties of monolithic ceramics at room temperature – part 6: guidance for fractographic investigation (german version). DIN, Berlin; 2009.
[3] ASTM-C1678-10. Practice for fractographic analysis of fracture mirror sizes in ceramics and glasses. ASTM International; 2010.
[4] Fréchette VD. Failure analysis of brittle materials. Advances in ceramics, vol. 28. Westerville, Ohio: The American Ceramic Society; 1990.
[5] Freiman SW, Mecholsky JJJ. The fracture of brittle materials: testing and analysis. first edition Hoboken, New Jersey, USA: The American Ceramic Society. Published by John Wiley & Sons, Inc.; 2012.
[6] Varner J. Descriptive fractography. In: Schneider SJ, editor. Ceramics and glasses, vol 4, engineering materials handbook. Metals Park, Ohio: ASM International; 1991. p. 635–44.
[7] Hull D. Factography observing, measuring and interpreting fracture surface topography. Cambridge University Press; 1999.
[8] Quinn GD. A NIST recommended practice guide: fractography of ceramics and glasses. Special publication 960-16e2. Washington, DC: National Institute of Standards and Technology; 2016 http://nvlpubs.nist.gov/nistpubs/specialpublications/NIST.SP.960-16e2.pdf.
[9] Kelly JR, Campbell SD, Bowen HK. Fracture-surface analysis of dental ceramics. J Prosthet Dent 1989;62:536–41.
[10] Kelly JR, Giordano R, Pober R, Cima MJ. Fracture surface analysis of dental ceramics: clinically failed restorations. Int J Prosthodont 1990;3:430–40.
[11] Quinn JB, Quinn GD, Kelly JR, Scherrer SS. Fractographic analyses of three ceramic whole crown restoration failures. Dent Mater 2005;21:920–9.

[12] Scherrer SS, Quinn GD, Quinn JB. Fractographic failure analysis of a Procera AllCeram crown using stereo and scanning electron microscopy. Dent Mater 2008;24:1107–13.
[13] Scherrer SS, Quinn JB, Quinn GD, Kelly JR. Failure analysis of ceramic clinical cases using qualitative fractography. Int J Prosthodont 2006;19:185–92.
[14] Scherrer SS, Quinn JB, Quinn GD, Wiskott HW. Fractographic ceramic failure analysis using the replica technique. Dent Mater 2007;23:1397–404.
[15] Lohbauer U, Amberger G, Quinn GD, Scherrer SS. Fractographic analysis of a dental zirconia framework: a case study on design issues. J Mech Behav Biomed Mater 2010;3:623–9.
[16] Lohbauer U, Belli R, Arnetzl G, Scherrer SS, Quinn GD. Fracture of a veneered-ZrO_2 dental prosthesis from an inner thermal crack. Case Studies Eng Fail Anal 2014;2:100–6.
[17] Belli R, Scherrer SS, Reich S, Petschelt A, Lohbauer U. In vivo shell-like fractures of veneered-ZrO_2 fixed dental prostheses. Case Studies Eng Fail Anal 2014;2:91–9.
[18] Du Q, Swain MV, Zhao K. Fractographic analysis of anterior bilayered ceramic crowns that failed by veneer chipping. Quintessence Int 2014;45:369–76.
[19] Gahlert M, Burtscher D, Grunert I, Kniha H, Steinhauser E. Failure analysis of fractured dental zirconia implants. Clin Oral Implants Res 2012;23:287–93.
[20] Moraguez OD, Wiskott HW, Scherrer SS. Three- to nine-year survival estimates and fracture mechanisms of zirconia- and alumina-based restorations using standardized criteria to distinguish the severity of ceramic fractures. Clin Oral Investig 2015;19:2295–307.
[21] Oilo M, Gjerdet NR. Fractographic analyses of all-ceramic crowns: a study of 27 clinically fractured crowns. Dent Mater 2013;29:e78–84.
[22] Oilo M, Hardang AD, Ulsund AH, Gjerdet NR. Fractographic features of glass-ceramic and zirconia-based dental restorations fractured during clinical function. Eur J Oral Sci 2014;122:238–44.
[23] Waddell JN, Payne AG, Swain MV, Kieser JA. Scanning electron microscopy observations of failures of implant overdenture bars: a case series report. Clin Implant Dent Relat Res 2010;12:26–38.
[24] Wolfart S, Harder S, Eschbach S, Lehmann F, Kern M. Four-year clinical results of fixed dental prostheses with zirconia substructures (Cercon): end abutments vs. cantilever design. Eur J Oral Sci 2009;117:741–9.
[25] Basilio Mde A, Delben JA, Cesar PF, Rizkalla AS, Santos Junior GC, Arioli Filho JN. Failure modes of Y-TZP abutments with external hex implant-abutment connection determined by fractographic analysis. J Mech Behav Biomed Mater 2016;60:187–94.
[26] Oilo M, Quinn GD. Fracture origins in twenty-two dental alumina crowns. J Mech Behav Biomed Mater 2016;53:93–103.
[27] Koenig V, Vanheusden AJ, Le Goff SO, Mainjot AK. Clinical risk factors related to failures with zirconia-based restorations: an up to 9-year retrospective study. J Dent 2013;41:1164–74.
[28] Taskonak B, Mecholsky Jr JJ, Anusavice KJ. Fracture surface analysis of clinically failed fixed partial dentures. J Dent Res 2006;85:277–81.
[29] Taskonak B, Yan J, Mecholsky Jr JJ, Sertgoz A, Kocak A. Fractographic analyses of zirconia-based fixed partial dentures. Dent Mater 2008;24:1077–82.
[30] Mecholsky Jr JJ. Fractography: determining the sites of fracture initiation. Dent Mater 1995;11:113–6.
[31] Della Bona A, Mecholsky Jr JJ, Anusavice KJ. Fracture behavior of lithia disilicate- and leucite-based ceramics. Dent Mater 2004;20:956–62.
[32] Belli RS, S.S.;Lohbauer U. Report on fractures of trilayered all-ceramic fixed dental prostheses. Case Studies Eng Fail Anal 2016;7:71–9.
[33] Thompson JY, Anusavice KJ, Naman A, Morris HF. Fracture surface characterization of clinically failed all-ceramic crowns. J Dent Res 1994;73:1824–32.
[34] Denry I. How and when does fabrication damage adversely affect the clinical performance of ceramic restorations? Dent Mater 2013;29:85–96.
[35] Scherrer SS, Cattani-Lorente M, Yoon S, Karvonen L, Pokrant S, Rothbrust F, et al. Post-hot isostatic pressing: a healing treatment for process related defects and laboratory grinding damage of dental zirconia? Dent Mater 2013;29:e180–90.
[36] Quinn JB, Quinn GD. A practical and systematic review of Weibull statistics for reporting strengths of dental materials. Dent Mater 2010;26:135–47.
[37] Quinn GD, Hoffman K, Quinn JB. Strength and fracture origins of a feldspathic porcelain. Dent Mater 2012;28:502–11.
[38] Della Bona A, Anusavice KJ, DeHoff PH. Weibull analysis and flexural strength of hot-pressed core and veneered ceramic structures. Dent Mater 2003;19:662–9.
[39] Basso GR, Moraes RR, Borba M, Griggs JA, Della Bona A. Flexural strength and reliability of monolithic and trilayer ceramic structures obtained by the CAD-on technique. Dent Mater 2015;31:1453–9.
[40] Borba M, de Araujo MD, de Lima E, Yoshimura HN, Cesar PF, Griggs JA, et al. Flexural strength and failure modes of layered ceramic structures. Dent Mater 2011;27:1259–66.
[41] Borba M, de Araujo MD, Fukushima KA, Yoshimura HN, Cesar PF, Griggs JA, et al. Effect of the microstructure on the lifetime of dental ceramics. Dent Mater 2011;27:710–21.
[42] Scherrer SS, Cattani-Lorente M, Vittecoq E, de Mestral F, Griggs JA, Wiskott HW. Fatigue behavior in water of Y-TZP zirconia ceramics after abrasion with 30 mum silica-coated alumina particles. Dent Mater 2011;27:e28–42.
[43] Cesar PF, Della Bona A, Scherrer SS, Tholey MJ, van Noort R, Vichi A, et al. ADM guidance—ceramics: fracture toughness testing and method selection. Dent Mater 2017, http://dx.doi.org/10.1016/j.dental.2017.03.006.
[44] ASTM-C1421-01b. Standard test methods for determination of fracture toughness of advanced ceramics at ambient temperature. ASTM International; 2001.
[45] Newman JC, Raju IS. An empirical stress-intensity factor equation for the surface crack. Eng Fract Mech 1981;15:185–92.
[46] Cesar PF, Yoshimura HN, Miranda WG, Goldenstein H, Okada CY, Gonzaga CC. Fracture toughness of dental porcelains. J Dent Res 2003;82. B121-B.
[47] Cesar PF, Yoshimura HN, Miranda WG, Miyazaki CL, Muta LM, Rodrigues LE. Relationship between fracture toughness and flexural strength in dental porcelains. J Biomed Mater Res B 2006;78b:265–73.
[48] Scherrer SS, Kelly JR, Quinn GD, Xu K. Fracture toughness (K_{Ic}) of a dental porcelain determined by fractographic analysis. Dent Mater 1999;15:342–8.
[49] Canneto JJ, Cattani-Lorente M, Durual S, Wiskott AH, Scherrer SS. Grinding damage assessment on four high-strength ceramics. Dent Mater 2016;32:171–82.
[50] Curran P, Cattani-Lorente M, Anselm Wiskott HW, Durual S, Scherrer SS. Grinding damage assessment for CAD–CAM restorative materials. Dent Mater 2017:294–308.
[51] Mallmann F, Rosa L, Borba M, Della Bona A. Effect of screw-access hole and mechanical cycling on fracture load of three-unit implant-supported fixed dental prostheses. J Prosthet Dent 2017 (accepted for publication).

[52] Fischer H, Karaca F, Marx R. Detection of microscopic cracks in dental ceramic materials by fluorescent penetrant method. J Biomed Mater Res 2002;61:153–8.
[53] Lohbauer U, Scherrer SS, Della Bona A, Tholey MJ, van Noort R, Vichi A, et al. ADM guidance—ceramic: all-ceramic multilayer interfaces in dentistry. Dent Mater 2017, http://dx.doi.org/10.1016/j.dental.2017.03.005.
[54] Benetti P, Kelly JR, Sanchez M, Della Bona A. Influence of thermal gradients on stress state of veneered restorations. Dent Mater 2014;30:554–63.
[55] Guazzato M, Walton TR, Franklin W, Davis G, Bohl C, Klineberg I. Influence of thickness and cooling rate on development of spontaneous cracks in porcelain/zirconia structures. Aust Dent J 2010;55:306–10.
[56] Swain MV. Unstable cracking (chipping) of veneering porcelain on all-ceramic dental crowns and fixed partial dentures. Acta Biomater 2009;5:1668–77.
[57] Zhang Z, Guazzato M, Sornsuwan T, Scherrer SS, Rungsiyakull C, Li W, et al. Thermally induced fracture for core-veneered dental ceramic structures. Acta Biomater 2013;9:8394–402.
[58] Zhang Z, Zhou S, Li Q, Li W, Swain MV. Sensitivity analysis of bi-layered ceramic dental restorations. Dent Mater 2012;28:e6–14.
[59] Zhang Y, Allahkarami M, Hanan JC. Measuring residual stress in ceramic zirconia-porcelain dental crowns by nanoindentation. J Mech Behav Biomed Mater 2012;6:120–7.
[60] Tholey MJ, Swain MV, Thiel N. Thermal gradients and residual stresses in veneered Y-TZP frameworks. Dent Mater 2011;27:1102–10.
[61] Mainjot AK, Najjar A, Jakubowicz-Kohen BD, Sadoun MJ. Influence of thermal expansion mismatch on residual stress profile in veneering ceramic layered on zirconia: measurement by hole-drilling. Dent Mater 2015;31:1142–9.
[62] Mainjot AK, Schajer GS, Vanheusden AJ, Sadoun MJ. Influence of cooling rate on residual stress profile in veneering ceramic: measurement by hole-drilling. Dent Mater 2011;27:906–14.
[63] Mainjot AK, Schajer GS, Vanheusden AJ, Sadoun MJ. Residual stress measurement in veneering ceramic by hole-drilling. Dent Mater 2011;27:439–44.
[64] Mainjot AK, Schajer GS, Vanheusden AJ, Sadoun MJ. Influence of zirconia framework thickness on residual stress profile in veneering ceramic: measurement by hole-drilling. Dent Mater 2012;28:378–84.
[65] Mainjot AK, Schajer GS, Vanheusden AJ, Sadoun MJ. Influence of veneer thickness on residual stress profile in veneering ceramic: measurement by hole-drilling. Dent Mater 2012;28:160–7.
[66] Fukushima KA, Sadoun MJ, Cesar PF, Mainjot AK. Residual stress profiles in veneering ceramic on Y-TZP, alumina and ZTA frameworks: measurement by hole-drilling. Dent Mater 2014;30:105–11.
[67] Wendler M, Belli R, Petschelt A, Lohbauer U. Characterization of residual stresses in zirconia veneered bilayers assessed via sharp and blunt indentation. Dent Mater 2015;31:948–57.
[68] Wendler M, Belli R, Petschelt A, Lohbauer U. Spatial distribution of residual stresses in glass-ZrO_2 sphero-cylindrical bilayers. J Mech Behav Biomed Mater 2016;60:535–46.
[69] Belli R, Petschelt A, Lohbauer U. Thermal-induced residual stresses affect the fractographic patterns of zirconia-veneer dental prostheses. J Mech Behav Biomed Mater 2013;21:167–77.
[70] Zhang Y, Sailer I, Lawn BR. Fatigue of dental ceramics. J Dent 2013;41:1135–47.